

Portland State University

PDXScholar

Dissertations and Theses

Dissertations and Theses

5-1-1970

Non-linearities in galvanomagnetic effects in bismuth at low temperatures

David Lawrence Luce
Portland State University

Follow this and additional works at: https://pdxscholar.library.pdx.edu/open_access_etds

Let us know how access to this document benefits you.

Recommended Citation

Luce, David Lawrence, "Non-linearities in galvanomagnetic effects in bismuth at low temperatures" (1970). *Dissertations and Theses*. Paper 646.
<https://doi.org/10.15760/etd.646>

This Thesis is brought to you for free and open access. It has been accepted for inclusion in Dissertations and Theses by an authorized administrator of PDXScholar. Please contact us if we can make this document more accessible: pdxscholar@pdx.edu.

AN ABSTRACT OF THE THESIS OF David Lawrence Luce for the Master
of Arts in Physics presented May 20, 1970.

Title: Non-linearities in Galvanomagnetic Effects in Bismuth at
Low Temperatures.

APPROVED BY MEMBERS OF THE THESIS COMMITTEE:

[REDACTED]
Laird C. Brodie, Chairman

[REDACTED]
David W. McClure

[REDACTED]
Cecil E. Sanford

[REDACTED]
Raymond Sommerfeldt

[REDACTED]
Donald Wright

The magnetoresistance and Hall coefficient of two single
crystals of bismuth have been measured at liquid helium temperatures.
The purpose of the work was to investigate the non-linearities which
had previously been observed in the longitudinal and Hall voltages as
a function of current. In addition to continuous current measurements,
a pulsed DC technique was used in an attempt to discriminate between
the non-linear effects due to heating and a possible intrinsic current
dependence of the magnetoresistance and Hall coefficient. The time
dependence of both of these galvanomagnetic effects indicates that the

rate of heat dissipation from the crystal into the normal helium increases suddenly about 50 ms after the current is applied. For example, at 4.2 K, 15 kG, and 50 mA, the sample temperature first rises to a value 0.2 K above the bath temperature, and then falls to a steady state value 0.06 K above the bath temperature. The resistance using a continuous current correlates with the steady state value of the time dependent resistance. A possible indication of gravitational dependence of the lambda transition was seen. Both above and below the lambda point the results of the low duty cycle pulsed DC measurements indicate the existence of an intrinsic non-ohmic effect when heating is minimized. The change in the resistance is of the order of 1 part per thousand per mA. In the normal fluid, the total current dependence of the magnetoresistance and the Hall coefficient is expressible as the sum of the intrinsic current dependence and that due to heating.

NON-LINEARITIES IN GALVANOMAGNETIC EFFECTS IN BISMUTH
AT LOW TEMPERATURES

by

DAVID LAWRENCE LUCE

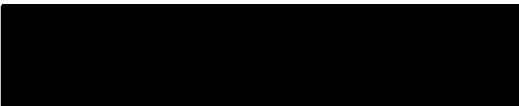
A thesis submitted in partial fulfillment of the
requirements for the degree of

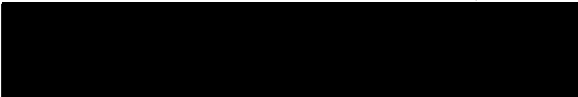
MASTER OF ARTS
in
PHYSICS

Portland State University
1970

TO THE OFFICE OF GRADUATE STUDIES:

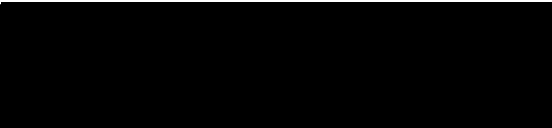
The members of the Committee approve the thesis of David
Lawrence Luce presented May 20, 1970.


Laird C. Brodie, Chairman

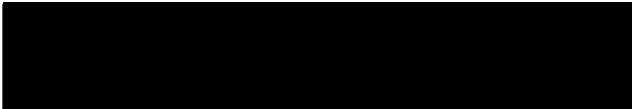

David W. McClure


Cecil E. Sanford


Raymond Sommerfeldt


Donald Wright

APPROVED:


Mark Gurevitch, Head, Department of Physics


Frank Roberts, Acting Dean of Graduate Studies

May 22, 1970

ACKNOWLEDGMENTS

The author wishes to express his sincere gratitude to Dr. Laird Brodie for his patient, painstaking guidance and help at every stage of this thesis. The suggestions and criticisms offered by Dr. Brodie have been essential to the conducting of the experiments and the writing of this report. The author also wishes to convey his thanks to his thesis committee for their patience and helpful comments.

Mr. Cecil Sanford first suggested a check on the current dependence of the resistance. In addition, the following students have contributed in many capacities to the experimental measurements: Mr. Jerry Bakke, Mr. James Barter, Mr. Charles Hartley, Mr. Robert Hufschmid, Mr. Michael Johnson, Mr. William Lutz, Mr. Roger McGinnis, Mr. Arnold Moodenbaugh, Mr. William Nordgren, and Mr. Michael Shibahara. Mr. Shibahara was especially helpful in mounting the crystals and helping with some of the calculations. The science department shop headed by Mr. Janacek, and the electronics shop headed by Mr. Weeks have also rendered valuable assistance in the construction of the experimental equipment. Finally the author is happy to acknowledge the continual encouragement and selfless dedication of Mrs. Martha Luce who typed the entire thesis.

TABLE OF CONTENTS

	PAGE
ACKNOWLEDGMENTS.....	iii
LIST OF TABLES.....	vi
LIST OF FIGURES.....	vii
INTRODUCTION.....	1
Historical Preface.....	2
Other Non-linear Effects.....	3
Experimental Goals.....	4
PRELIMINARY DISCUSSION OF MEASUREMENTS.....	5
EQUIPMENT.....	10
Samples.....	10
Quality Mounting	
Experimental Environment.....	16
Electrical Circuitry.....	19
PROCEDURE.....	28
CALCULATIONS AND RESULTS.....	33
Introduction.....	33
Thermal Results.....	34
Non-thermal Non-linearity.....	51
Misalignment of Leads.....	53
Experimental Results and Interpretation.....	56

	PAGE
CONCLUSIONS AND RECOMMENDATIONS.....	68
Conclusions.....	68
Recommendations.....	68
Thermal Non-linearity	
Non-thermal Effect	
A SELECTED BIBLIOGRAPHY.....	71
APPENDIX A.....	73
APPENDIX B.....	75
APPENDIX C.....	76

LIST OF TABLES

TABLE	PAGE
I Summary of Quality Measures	14

LIST OF FIGURES

FIGURE	PAGE
1. Representative Hall sample.....	1
2. Model for the Hall effect.....	5
3. Net electron paths if Hall field, E_H , applied electric field E_L , and magnetic induction are as shown.....	7
4. Crystal AA 209.....	12
5. Crystal AB 85.....	12
6. Experimental environment.....	17
7. Switch box circuit diagram.....	20
8. Typical rotation diagram, implying that the trigonal axis is at -15.3	21
9. Main circuit logic.....	22
10. Normal electrical connections.....	24
11. Pulse circuit diagram.....	25
12. Circuit diagram for amplifier box.....	29
13. Typical non-thermal normalization pulse.....	31
14. Typical non-thermal pulse, showing a negative ΔV	31
15. Potentiometric data at two temperatures.....	35
16. DC correlation on Hall leads.....	36
17. DC correlation (II).....	37
18. Anticipated time dependence of ΔV	38
19. Typical thermal ΔV	40
20. Typical long pulse at $T < T_\lambda$	40

21. Virgin pulse effect.....	43
22. Current dependence of peak. AA 209, Leads 4-3.....	47
23. The lambda sequence monotonically cooling.....	48
24. Effect on the Hall voltage of various degrees of misalignment.....	55
25. Typical set of four runs on leads 6-5.....	57
26. Typical set of four runs on leads 4-3.....	58
27. Diagram for model of leads 4-3, AB 85.....	59
28. Change in sign of R_T as current is varied.....	61
29. Current dependence of $\frac{\Delta R_T}{R_T}$ at various temperatures.....	62
30. Current dependence of non-thermal non-linearity.....	63
31. Temperature dependence of $\frac{\Delta R_T}{R_T}$	66
32. Temperature dependence of $\frac{\Delta R_T}{R_T}$	67
33. Dimensions for average temperature calculation.....	73
34. Dimensions for self field calculation.....	75

INTRODUCTION

When an electric field, \vec{E} , is applied parallel to the long dimension of a metal rod, a current, I , is produced in the rod as shown in Figure 1. The ratio of the longitudinal potential difference, V_L , to the current is defined as the electrical resistance R .

If a magnetic field is applied normally to the broad face of the sample, the resistance increases, and this change in R is called the magnetoresistance.

In the absence of the magnetic field the transverse voltage between points a and b is zero under most conditions. Thus \overleftrightarrow{ab} is an equipotential. However, in 1879 E.H. Hall (1) discovered that a transverse potential

difference, V_H , appears when the magnetic field is turned on. This observation implies that the application of the magnetic field results in a rotation of the equipotentials. The Hall

voltage, V_H , is normally found to be proportional to the magnetic induction, \vec{B} , and to the current, and inversely proportional to the thickness of the sample, d . Therefore, a Hall coefficient R_H is defined as $R_H = \frac{Vd}{I|\vec{B}|}$ for the geometry of Figure 1.

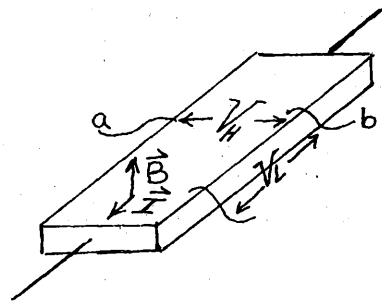


Figure 1. Representative Hall sample.

Ordinarily the resistance, magnetoresistance, and Hall coefficient are independent of current if B and the specimen temperature are held constant. Thus, under these conditions V_L and V_H are linear functions of the current. However, it is the purpose of this thesis to report some non-linearities in V_L and V_H which have been observed in bismuth single crystals at liquid helium temperatures. The sensitivity of both the magnetoresistance and the Hall coefficient to changes in the temperature suggests that the non-linearities which are observed may include some components which are due to temperature changes in the crystal. However, these experiments indicate an additional component in the observed non-linearity which appears to be non-thermal in nature.

Historical Preface

The phenomena discussed in this dissertation first came to light during a routine check of the assumption of Ohm's law behavior of crystal voltages preparatory to a study of the effects of trace impurities on the galvanomagnetic properties of bismuth. It was noted that when either the magnetoresistance or the Hall coefficient was measured potentiometrically, it was not independent of current. Since the direction of the changes was the same at 4.2 K as one would expect from crystal heating, it was postulated that the thermal resistance of some part of the system- the sample, the bath, or the interface between the two- was allowing the sample to warm due to Joule heating. The coefficient in question would then be character-

istic of a temperature somewhat higher than that indicated by the manometer vapor pressure reading. To decide between the possibilities two courses were taken. First a calculation (see Appendix A) of the amount by which the average sample temperature could increase above the bath temperature when the surface was held at the temperature of the liquid was made. Even using the minimum thermal conductivity available for bismuth at low temperatures, the resultant possible temperature elevation due to Joule heating and the thermal resistance was too small by one or two orders of magnitude. Furthermore, when the bath was cooled to the lambda point, there was a dramatic discontinuity in the values of the non-linearities of all the coefficients, and for the Hall coefficient a change in sign of the perturbation. Since the thermal conductivity of the liquid helium increases by several orders of magnitude at the lambda point it was concluded that the thermal contribution to the non-linearity was due to thermal resistance in the bath. However, since the crystal could not support a large thermal gradient, and since the non-linearity still existed below the lambda point, there appeared to be an additional non-thermal contribution to the non-linearity.

Other Non-linear Effects

Departures from a linear relation between current and voltage, have been observed elsewhere, and ascribed to several phenomena. Esaki (2) found a sudden change in the slope of the I-V curve for exactly this situation of perpendicular electric and magnetic fields, at a ratio of electric to magnetic field of about 10^5 cm/s. Since

the maximum ratio for our experiments was less than 2×10^4 cm/s, his "kink" would not have been seen in our present experiments. Also often mentioned are the various self-induced field effects, in which the magnetic field produced by the current appreciably augments the external field (3). Again, these effects are for far larger currents than those we were using. A calculation has been made, (see Appendix B), which indicates that the maximum self magnetic field for our case is on the order of two parts per million. Such a small addition to the magnetic field would not produce noticeable effects with our present equipment.

Experimental Goals

The primary experimental goal was to separate the thermal effects from the postulated intrinsic non-linearity. Any intrinsic effect was expected to respond to current changes much more quickly than a thermal effect. Therefore the observation of the longitudinal and Hall voltages as a function of time could be used to effect the separation. An apparatus was constructed to produce and read DC pulses of variable widths and repetition rates. Long pulses or direct current could be used to examine the progress of heating, and short pulses could be used if heating were to be minimized.

PRELIMINARY DISCUSSION OF MEASUREMENTS

As was pointed out by Hall (1), the effect bearing his name can be understood from a free electron model. In the absence of the magnetic field the current, I , consists of electrons which have a net drift velocity in the direction of the electric field. When the magnetic field is applied the Lorentz force generates a net force on the electrons toward one side of the sample (Figure 2). If there is no electrical connection from the overpopulated side to the depleted side, an electric field \vec{E}_H builds up, which deflects the carriers back to their original path. Thus the current remains the

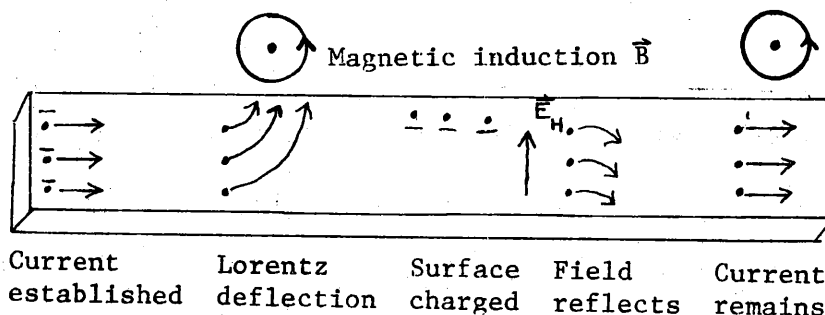


Figure 2. Model for the Hall effect, after Ziman (4).

same, but an additional voltage, V_H , is added transverse to both the current and magnetic field, which is proportional to current for low currents and fields. A coefficient is therefore defined, for the purposes of this paper, as $R_T = V_H/I$. It may be noted that the Hall

coefficient, defined as $R_H = \frac{V_H d}{IB}$, is proportional to this "transverse resistance" at constant magnetic field and sample thickness. It is experimentally observed that R_T decreases as temperature increases.

In the above discussion the implication that the current remains unchanged in the longitudinal direction is not realistic. To assist in the argument, let us refine our picture of transport in the crystal. We envisage the trajectory of a conduction electron in the absence of magnetic field as a random series of straight lines between collisions, with a net velocity in the direction of the applied electric field. However, these collisions are not with stationary ion cores, or other electrons, but with imperfections in the lattice, impurity atoms in normal sites, or phonons generated by thermal energy of the cores. In the absence of these collisions the electrons experience no resistance from collisions with the ion lattice itself, contrary to what one might expect from classical considerations.

In zero magnetic field this nearly free electron model gives the correct dependence of resistance in metals with temperature if one assumes that the population of thermal phonons is linear in temperature. At room temperature the phonon concentration for a reasonably good crystal is much greater than the imperfection and impurity concentrations, and so the resistance is almost linear in temperature. At low temperatures, though, thermal phonons are so few that their density is close to that of the impurities and the imperfections, and the resistance goes to a constant value (residual

resistance).

When a magnetic field is applied, the dependence of the resistance on scattering is reversed. Under the influence of crossed electric and magnetic fields the carriers traverse the crystal with a net drift path in the shape of a trochoid (Figure 3a). The average displacement of the carrier is perpendicular to the electric field, \vec{E} , which is the sum of the applied longitudinal field, \vec{E}_L , and the Hall field \vec{E}_H . Since \vec{E}_H is usually small compared to \vec{E}_L , \vec{E} is nearly parallel to \vec{E}_L , and the carriers make only slight progress in the direction of \vec{E}_L .

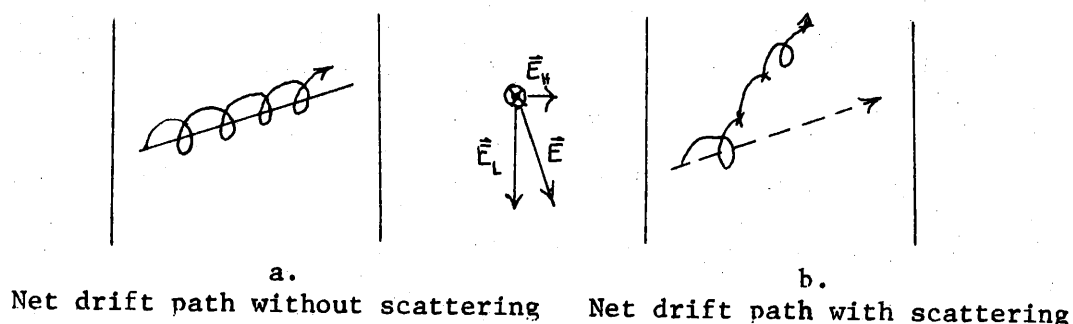


Figure 3. Net electron paths if Hall field, \vec{E}_H , applied electric field, \vec{E}_L , and magnetic induction are as shown.

When a collision occurs, the carrier is knocked out of its orbit, (Figure 3b), and this is the basic mechanism which allows conduction. After the collision, the low velocity part of the path is determined more by the electric force than the magnetic, and an enhanced drift velocity in the electric field direction results.

Again this model gives a qualitatively correct dependence of magnetoresistance on temperature, with the same assumption that the

phonon population is linear in temperature. Since the magnetoconductance is proportional to the number of scattering centers, the magnetoresistance shows an approximately inverse temperature dependence, similar to that of the Hall coefficient.

Parenthetically it should be noted that the thermal and thermoelectric effects normally associated with electric currents are also profoundly modified when a magnetic field is applied. One of the most well-known thermal transport effects is the Peltier effect, in which the action of an electric current produces a temperature difference between two junctions of dissimilar metals. This temperature gradient is superimposed on the temperature distribution resulting from Joule heating.

In addition to modifying the Peltier effect and changing the Joule heat, the application of a magnetic field produces a transverse temperature gradient in a sample carrying an electric current. The appearance of this temperature gradient is called the Ettingshausen effect. The reason for mentioning these effects is that not only is the bismuth crystal an excellent macroscopic thermometer, but it seems to form a highly sensitive differential thermometer as well. If a temperature difference is produced between a pair of junctions of dissimilar metals, a voltage appears (the Seebeck effect), and since the potential leads attached to the bismuth are copper, the requisite junctions exist. The high resolution of the amplifier system allows us to record any such thermocouple voltage, and from that voltage we may infer the existence of a temperature gradient in the crystal.

It was expected that each Seebeck voltage would appear as an exponentially decaying tail after the current was turned off, because of the long thermal relaxation time. Hence, the presence of such tails on the scope trace would indicate any inhomogeneity in the crystal warming.

EQUIPMENT

Samples

Quality. The effects described in this paper were observed in two separate single crystals with a number of independent pairs of leads on each. In assessing the pertinence of these results for elemental bismuth, it is appropriate to spend some time discussing crystal quality.

Crystal quality is not always exactly specifiable, because there is more than one way of being "good". A high impurity concentration, though, would indicate a poor crystal. Since, as argued above, resistance to electron flow is due in part to impurity and imperfection scattering, the most direct measure of quality would be the resistance near absolute zero. Since all non-superconductors tend to go to a "residual resistance" at some temperature above absolute zero the ratio of this resistance to that at some other temperature, say room temperature would also be a quality measure. Finally, since only a few sets of leads on one of the crystals we are dealing with, have gone to a condition where $dR/dT = 0$ at temperatures available to us, the best measure we have is to take a ratio between resistance at room temperature and that at either 4.2 K or at the lowest available temperature, which is about 1.5 K.

Also, as discussed in the previous section, the effect of scattering centers is to increase the conductivity in a magnetic field. Therefore one could use the ratio of zero field conductivity to the

conductivity at some specified field as a measure of imperfection concentration, and its inverse as a figure of merit.

Other measures of quality include light figures, that is, reflections from the sides of etch pits, which are used to determine orientation of the crystallographic axis with respect to the geometry of the bulk crystal. Each crystal is also judged by optical means for obvious defects, such as "striations", which are small angle grain boundaries, and "strain bands", which are deformed areas resulting from distortion of the crystal. Malorientation or striations are defects in the growth of the crystal, and are usually cause for rejection and regrowing the crystal, while strain bands are usually the result of an accident after the crystal is cool, and are considered to be only local in effect.

AB 85 and AA 209, the two crystals used for these experiments, were single crystals of good quality. AA 209 was cast of Cominco bismuth of 69 purity grade, and zone grown; AB 85 was made of 59 grade metal from Cerro de Pasco, and recrystallized 11 times. Both used seeds with the trigonal crystal axis perpendicular to the broad face of the plank-shaped crystal, (Figures 4 and 5). If the plank were set on end, the three binary axes would form a balanced equilateral triangle in the plane of the broad face.

The crystal on which the pulser and amplification system (See below) was first used was AA 209, (Figure 4). This crystal is physically dimensioned approximately 1.5 mm thick by 5.4 mm wide, and is about 10 cm long. Its superficial shape is fairly rectangular, and it does not exhibit either striations or strain bands. The various

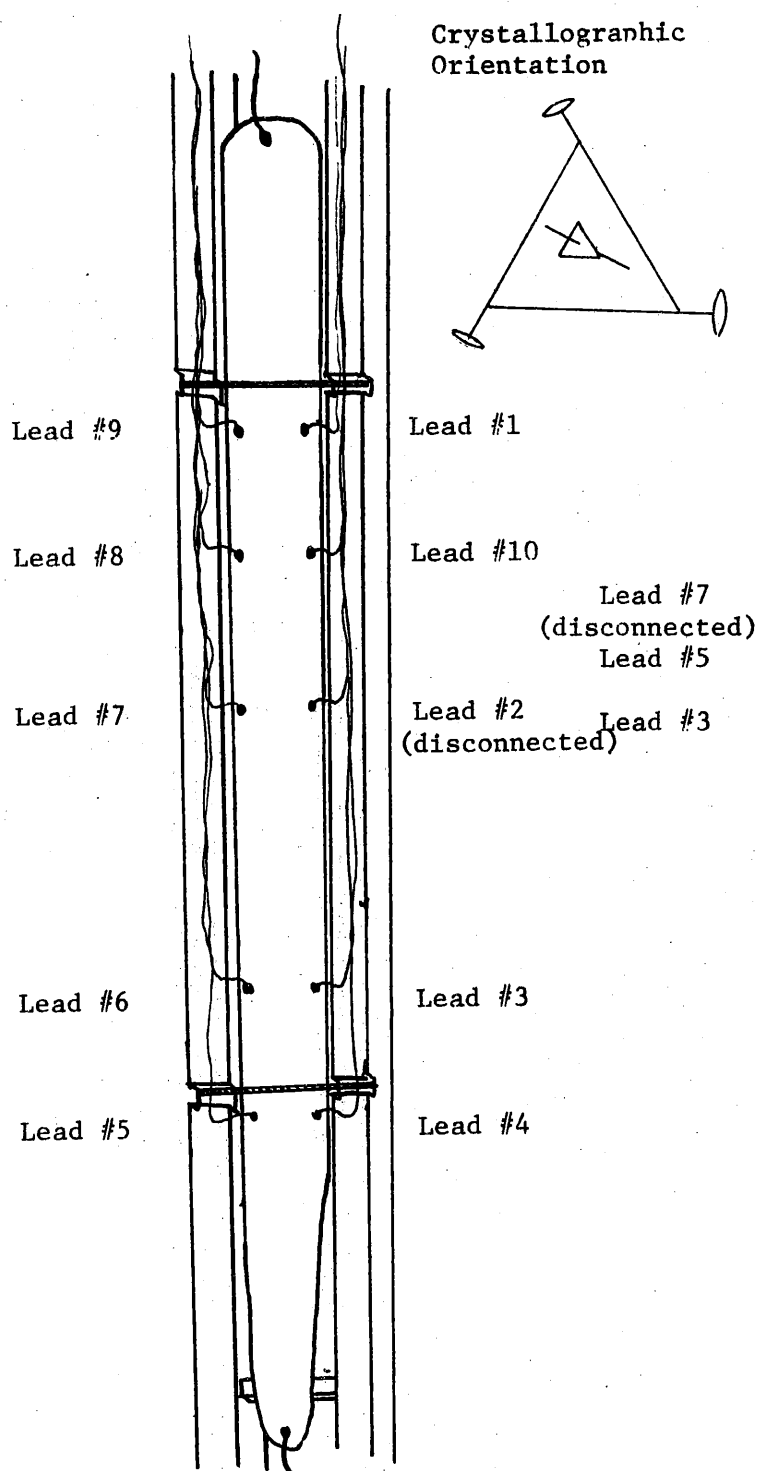


Figure 4. Crystal AA 209.

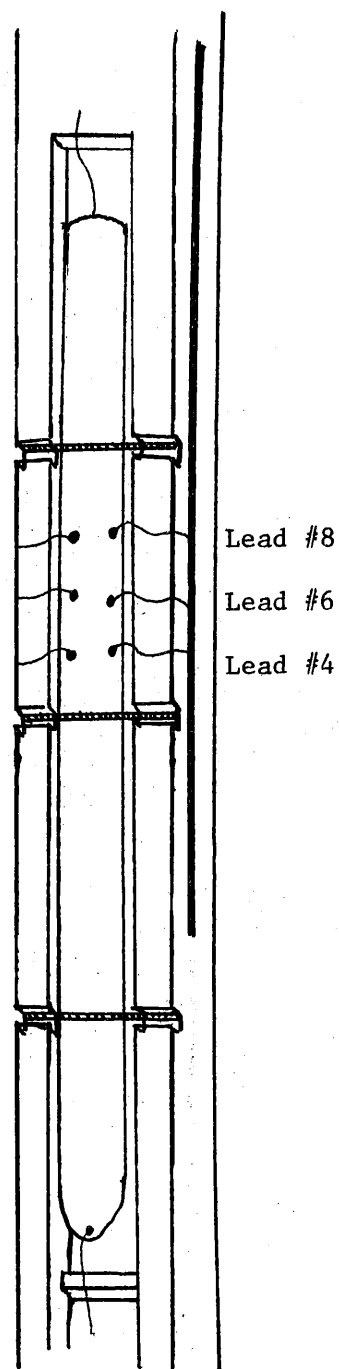


Figure 5. Crystal AB 85.

figures of merit are catalogued in Table I for both crystals and, for comparison, a set of values from the literature which are considered good in bismuth single crystals.

AB 85 was the second of the two crystals to be measured by pulsing, although extensive direct current measurements had been taken on it previously. As grown, it has a good, striation-free shape and is physically dimensioned as 1.7 mm by 4.85 mm by about 90 mm. The quality measures, as catalogued in Table I, are considered exceptional for bismuth. At the conclusion of the potentiometric measurements on it, AB 85 suffered an accident which introduced several strain bands. Upon replacement of the potential leads in the apparently strain free region, the ratios were remeasured, and found to be similar to those previous to the accident. Since this crystal still seemed superior to any of the other crystals measured, we felt confident in continuing measurements on it.

Mounting. Before the crystal is available for measurement, it must be mounted in a suitable support, both to prevent its motion in the field and to protect it from the vagaries of its environment. Also part of the mounting process is the attachment of leads to the crystal itself, and connecting it thusly to the external circuit.

The art of mounting is basically a compromise between maximum permanence and confinement and minimum likelihood of damage to the crystal. For instance, securing the crystal to the holder might be a good way of eliminating motion in the magnetic field, but overly tight bonds might strain it. Another consideration in mounting crystals for these studies was to provide as much area as possible for

TABLE I
SUMMARY OF QUALITY MEASURES

Crystal Number	AB 85	AA 209	Best Values in Literature
Technique	Grown from melt 11 times	Zone refined and Zone grown	Grown from melt 90 times (5)
$\frac{\rho(0.0)}{\rho(4.2,0)}$	530	460	590 (5)
$\frac{\rho(4.2,10)}{\rho(4.2,0)}$	4.5×10^6	2.3×10^6	
$\frac{\rho(0.0)}{\rho(1.5,0)}$	$>3.1 \times 10^3$	830	1180 (6)
Orientation -trigonal (HB) -binary (LJ)	2° 2/3°, 1/4°, 1°	1° 1/2°, 1/4°, 1/2°	1° (5)

- All resistivities are $\rho(T, B)$.
- $T = 0$ implies Celsius degrees, otherwise Kelvins
- H is in kilogauss
- All crystals were grown with the trigonal axis \perp to the face.
- All crystals were grown with the binary axis \perp to the length.

heat exchange between solid and bath. This prompted the open crystal mounts seen in Figures 4 and 5.

The current leads, for a four terminal measurement, are quite easy to connect. Since these leads are attached far from the experimental area, some thermal damage can be tolerated, and they may be soldered with bismuth to the ends of the crystal.

The potential leads are much more critical, since they are, of necessity, in the area which is to be measured. The details of the techniques are somewhat the subject of debate, but the procedure we have used is generally as follows:

1. Copper wire, AWG 44, is stripped chemically and pre-coated with bismuth.
2. A micrometer drive positions the lead and supplies a small amount of tension against the crystal.
3. A capacitor, charged to about 100 volts is discharged through a transformer into the lead-crystal junction, which lightly welds the copper into the bismuth.
4. The position of the lead is measured by a traveling microscope, and the lead is glued to the holder, leaving only enough spare to allow for differential expansion.

In most cases, the leads are placed from 5 to 10 mm apart, as close as possible to the edge of the crystal, and as nearly transverse to each other as may be managed.

Experimental Environment

The magnetic field in which the measurements were taken is supplied by a Varian 2503 12 inch electromagnet with a Fieldial power supply, found to be within specifications by nuclear magnetic resonance checks. The field thus supplied was checked in 1964 and found to be uniform to within about one gauss across a seven centimeter circle in which our crystal is centered.

The temperature environment is provided by a double dewar system, (Figure 6), constructed by Scanlon of California (7). A large volume Kinney pump is connected to lower the vapor pressure and hence the temperature of the helium bath. In addition, a covering flange was constructed for the nitrogen dewar in order to allow pumping on the boiling liquid to cool it and prevent its boiling during sensitive measurements. It was found that the boiling nitrogen bath was extremely sensitive to microphonics - when the table was bumped, more bubbles nucleated, and the general noise level in the crystal signals increased, as discussed more completely in the section on coherent noise.

The final part of the environment system is a pair of parallel manometers which provide a convenient temperature measurement. For high pressure measurement a mercury filled U tube was used, with a vacuum on one side of approximately 50 microns. At lower temperatures an oil filled manometer would be connected in parallel to the mercury one.

Since the lambda transition could be observed far more accurately using our electronic equipment than by observing the cessation

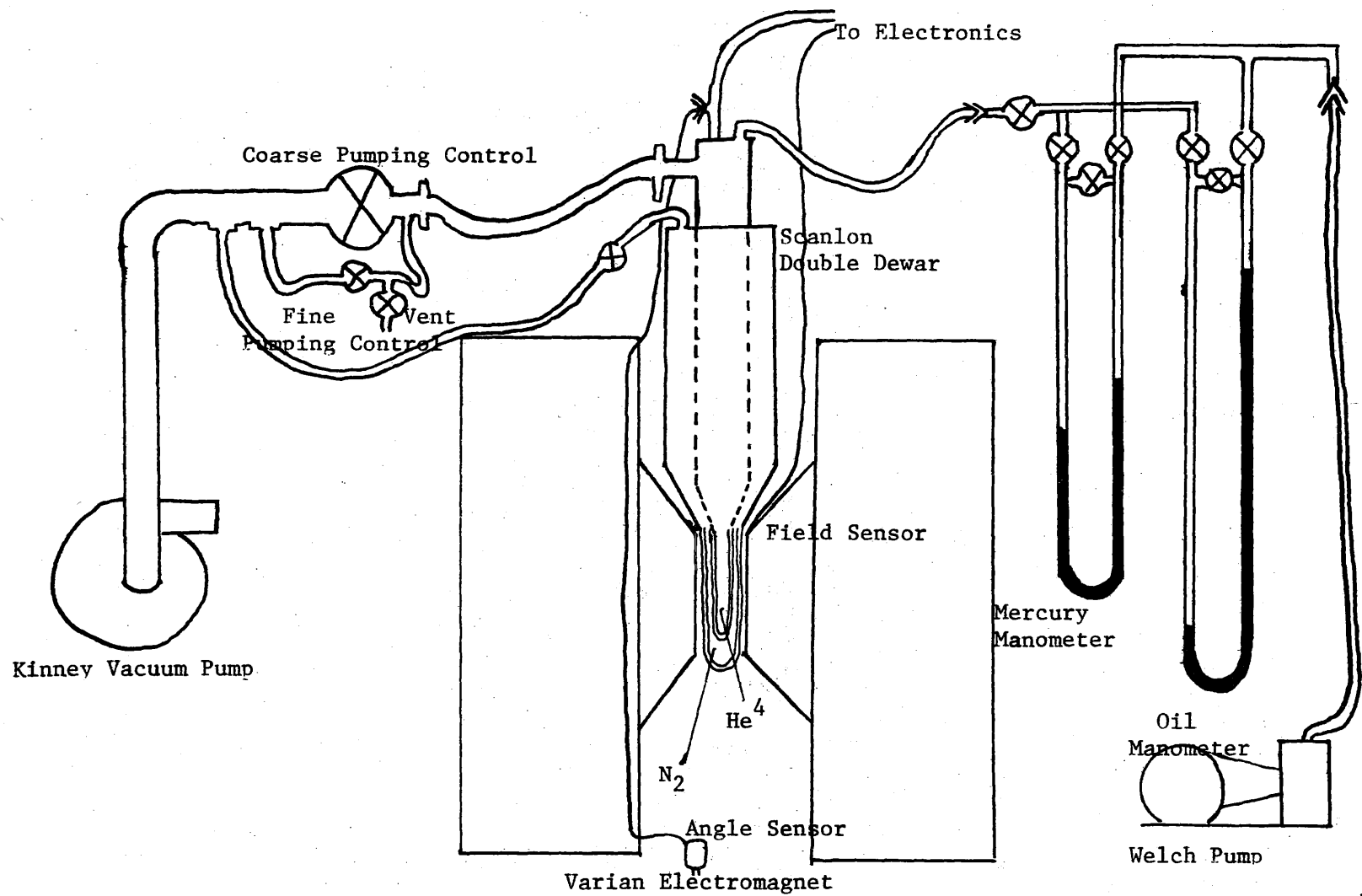


Figure 6. Experimental Environment.

of boiling in the helium, it was used to compute a conversion factor from oil to mercury. The lambda temperature, as given by Zemansky (8) was converted to a pressure in cm of mercury by using the National Bureau of Standards 1948 tables of helium saturated vapor pressure versus temperature. Since this pressure could be read in cm of oil, a ratio of oil density to mercury density was calculated, and each oil height could be converted into a mercury height. The mercury height was then correlated, by using the National Bureau of Standards tables, to a temperature. By this procedure it was found that the oil height was 13.68 times the mercury height.

Electrical Circuitry

One of the most important parameters in the experiments is the orientation of the magnetic field with respect to the crystallographic axes. To insure that the orientation was always the same, the magnetic field was moved until it was parallel to the trigonal axis. Since the crystals used were grown with the trigonal axis perpendicular to the flat face of the specimen, this direction of magnetic field would be the logical way to measure the Hall effect in the samples. To ascertain that this was indeed the axis of symmetry, longitudinal voltage was plotted versus angle of the magnet. From crystallographic considerations it was felt that the magneto-resistance should be symmetric about the trigonal axis. When such a graph displayed clear symmetry, the trigonal axis was taken to be in the plane described by the angle at which the reflection symmetry of the graph occurred.

To facilitate the plotting of this graph, the part of the electrical logic outlined by dots in Figure 7 was constructed. A ten-turn voltage divider was attached to the magnet so its shaft turned when the magnet rotated, and supplied with a voltage from the main batteries. A voltage, proportional to displacement angle could then be obtained from the center tap, and fed to the horizontal axis of a Hewlett Packard 7000A XY recorder. The ordinate is supplied straight from the magnetoresistance lead pair. The high input impedance of the recorder renders auxiliary amplifiers unnecessary and gives very nice-looking graphs with a minimum of effort, (Figure 8).

The main circuit, (Figure 9), is likewise simple, in concept if not in execution. A power source feeds an essentially constant, comparatively large voltage to a series circuit. The current in the circuit is limited by the large variable resistor R_L , and flows to a precision resistor R_M . The voltage across R_M , which is proportional to current, is amplified and displayed on an oscilloscope screen, as a function of time. R_S is a source of voltage which follows Ohm's law and which can be compared to the voltage from the crystal. Any non-linearity can then be displayed, by subtracting the linear voltage from R_S from the crystal voltage and, after appropriate amplification, displaying the difference on the same oscilloscope with respect to time.

The power for the circuit was always supplied by the same set of batteries, but the current could be channeled through a pulser, instead of directly to the crystal, so that it could be switched on

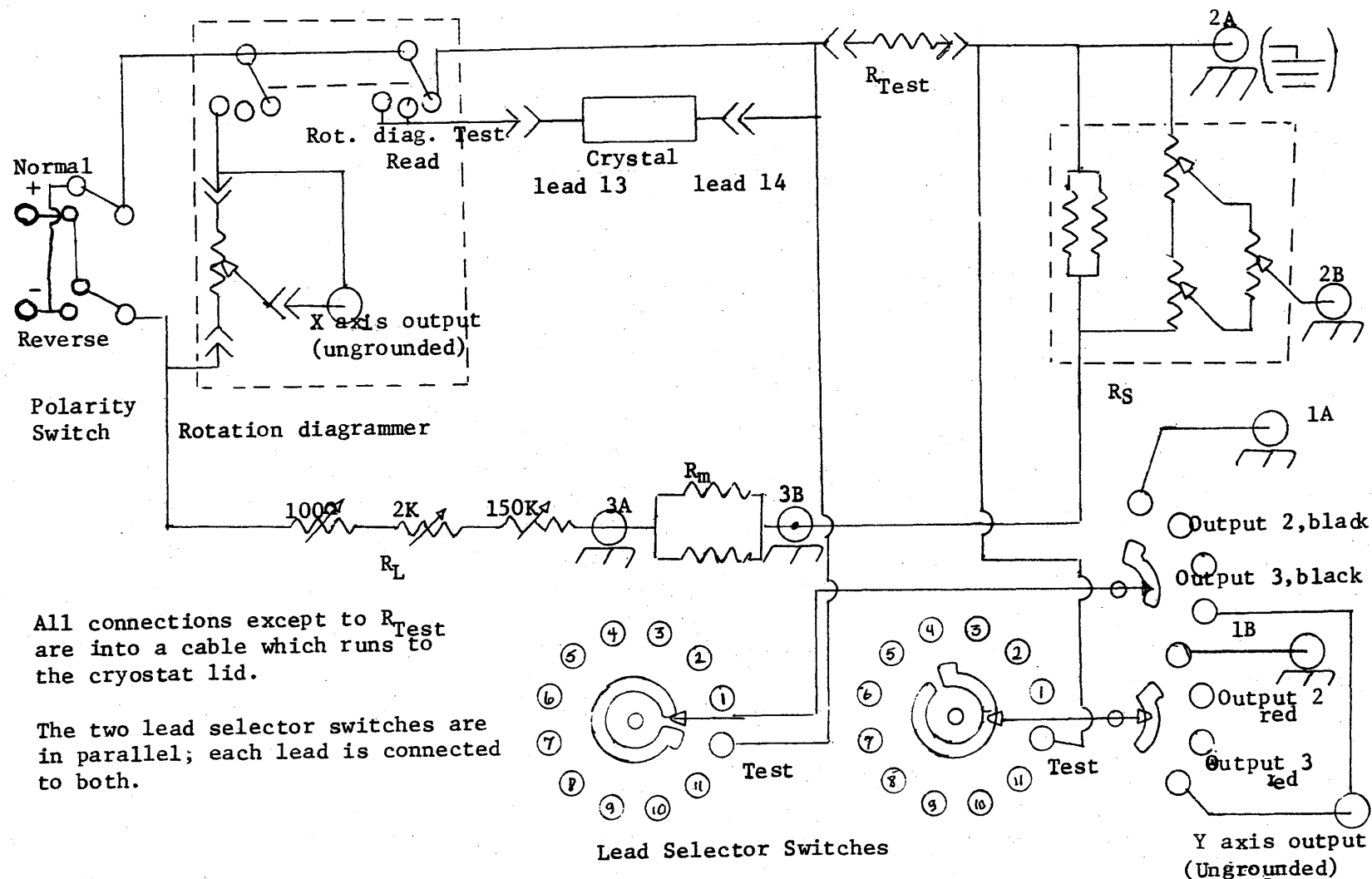


Figure 7. Switch box circuit diagram.

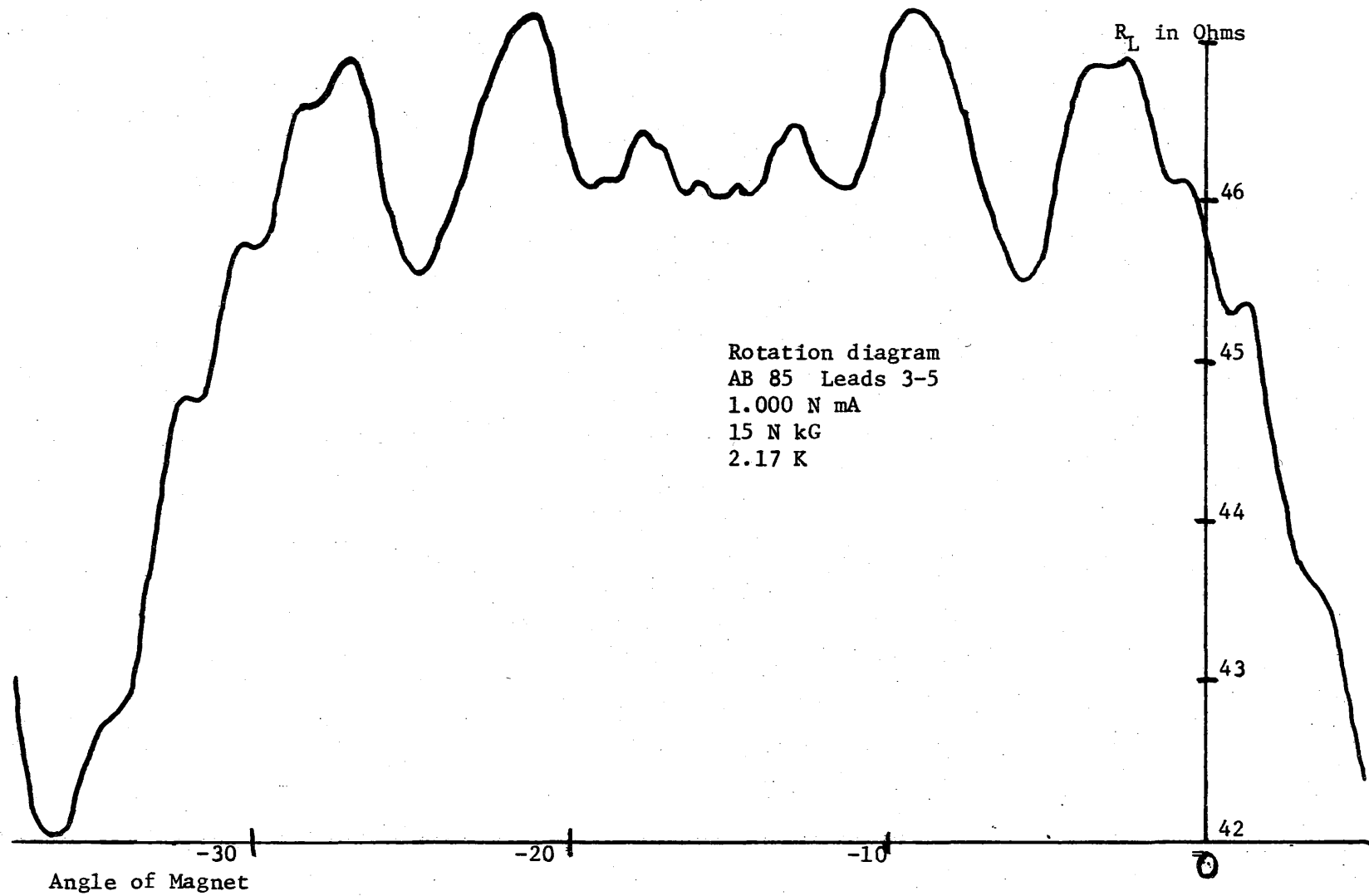


Figure 6. Typical rotation diagram, implying that the trigonal axis is at -15.5°

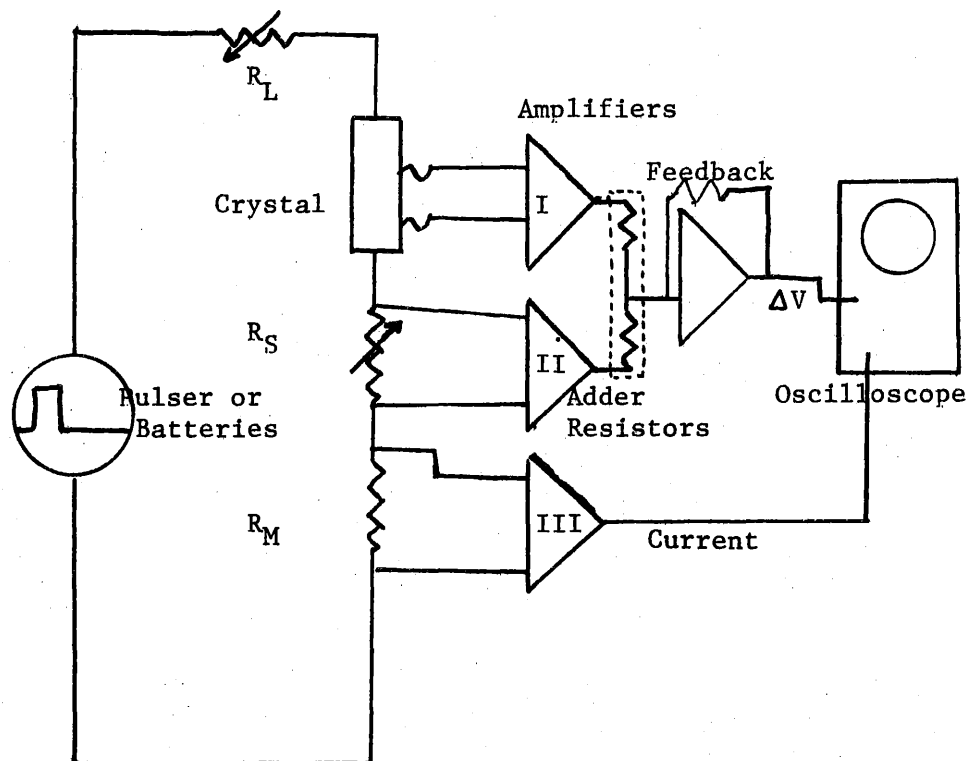


Figure 9. Main circuit logic.

automatically as well as manually. As a result of the pulser's peculiar internal connections, the switch from DC mode to pulsing mode had to be wired as in Figure 10. This allowed the pulser to continue operating at standby even when it was not connected to the crystal.

The pulser itself (Figure 11) is a small, separate unit which allows the operator to vary both the repetition rate of the pulse and its width. The repetition rate is set by a relaxation oscillator which has a unijunction transistor, T_1 , as its non-linear element. The output from this is capacitively coupled to a monostable switch circuit, T_2 , T_3 , and "flips" it to supply a voltage to the base of the output transistor, T_4 . A simple charging circuit resets (flops) the switch after a time determined by its RC time constant, and the switch in turn denies the voltage to the output transistor. At the operator's option, the final transistor may be connected directly to the circuit, or a relay may be used to cut down the output impedance, and insure against leakage current.

The pulse height is controlled by a set of large series resistors located in the switch box (Figure 7). A metal film resistor pair provides the standard (R_M) for measuring the current in the main loop. The voltage from R_M is fed to the input of amplifier three, a Burr Brown instrumentation amplifier model 3061, which is calibrated to give an output of one tenth of a volt for each mA of current.

To allow careful inspection of the non-linear part of the resistance, the plan was adopted to subtract the linear part and amplify

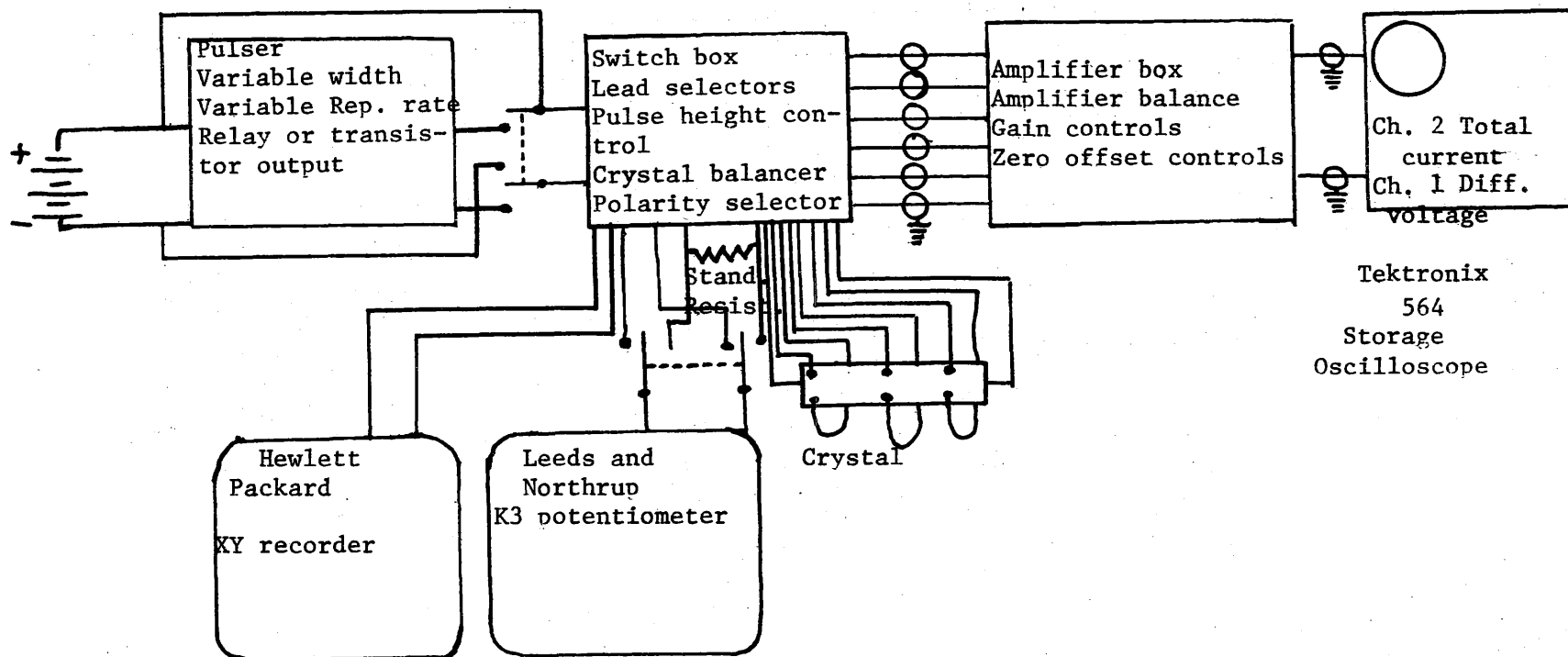


Figure 10. Normal electrical connections.

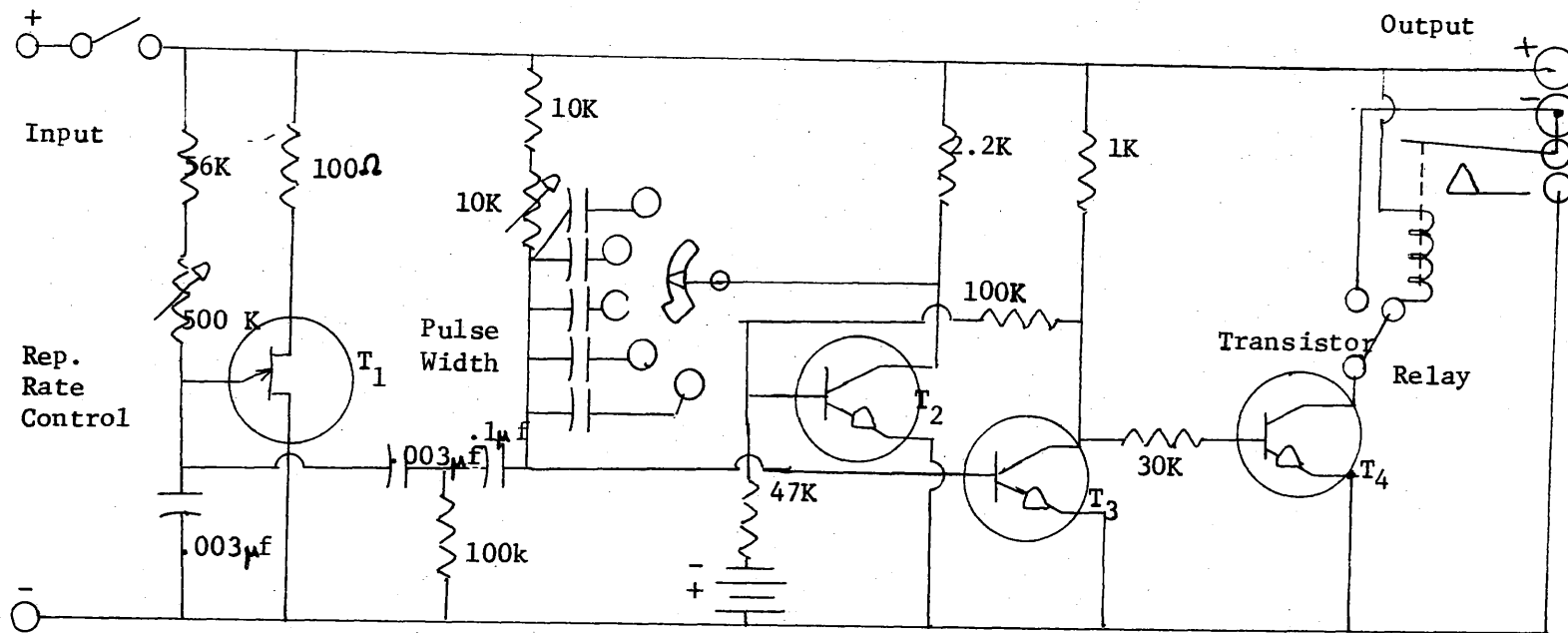


Figure 11. Pulser circuit diagram.

only the difference from linearity. When such a plan is adopted it is most important to make certain that effects in the standard R_S , Figure 7, do not mask or change the apparent behavior of the sample. Therefore, a metal film resistor, of low inductance and temperature coefficient of 25 parts per million per degree Celsius was adopted for the primary voltage source. In parallel with this a voltage divider was used to enable the operator to tune to exactly the crystal voltage at some current. Since a fine control was needed, the primary voltage divider was constructed of a pair of ganged ten-turn potentiometers, and a third ten-turn potentiometer was connected across their center taps. This symmetry was invoked to compensate for ambient temperature variations. The parallel voltage divider was used to minimize the inductance presented to the main flow of current. A final advantage was the availability of a wide range of ohmic voltages without loss of sensitivity.

The output from R_S is presented to the input of a Burr Brown instrumentation amplifier model 3061 (amp. 2, Figure 12) which is calibrated to a gain of 15. The voltage from the crystal leads under examination is sent to the input of a third Burr Brown 3061 (amp. 1, Figure 12) the gain of which was adjusted at the time of the reading to match precisely that of amp. 2. The outputs of these two amplifiers are subtracted, and the resultant voltage sent to the inverting input of the final amplifier (amp. 4, Figure 12), which is a Burr Brown model 3009, calibrated to a gain of 4. The 3061 amplifiers are differential types, with input impedances of approximately 50 Megohms and exceptional stability, while the 3009 is a

somewhat less sophisticated operational amplifier with an input impedance of about 500 kilohms.

Because of the short pulse lengths and variable duty cycle, the pulsed measurements employ an oscilloscope. We were fortunate to obtain the loan of a Tektronix storage scope model 564 which simplified the measurement process considerably. A sampling plug-in time base was used and triggered by the current pulse from amplifier three.

The voltage axis was supplied by a type 3A3 plug-in unit, which is an accurately calibrated dual trace set of differential amplifiers.

Each section of the measurement system was periodically checked with a Leeds and Northrup K-3 potentiometer. It was especially important to insure that the R_S gave a voltage linear in current, and it appeared to be so to at least a twentieth of a percent.

PROCEDURE

After transfer of the liquid helium, the first item of data taken was the so-called "rotation diagram". The magnetic field was rotated with respect to the crystal and magnetoresistive voltage plotted against angle. The magnet was set at the angle about which the graph was symmetric. Shifts of the crystal of up to 10 degrees were noted between runs, and it was felt these were the result of splashing as the liquid was transferred. Generally the crystal did not shift significantly with field reversal, violent bubbling or any other disturbance during each run.

Since the most important part of the data taking was precise comparison of the signal from the crystal with an ohmic signal, a careful procedure was employed to exactly set amplifiers 1 and 2 to identical gains. The first step was the calibration of amplifiers 2,3,and 4 to their respectively assigned gains. Zero offset adjustment was a part of this preliminary tuneup, but since that tended to drift, each reading had to be taken with respect to a zero voltage trace.

The first balance procedure, "amplifier balance", was intended to match the gains of channels 1 and 2 to the limit of the sensitivity of our equipment. The input leads of amplifiers 1 and 2 were tied together by a switch (S1, Figure 12), and a fairly large signal placed across them. The gain of amplifier 1 was then adjusted for a zero amplitude difference pulse to within the level allowed by the

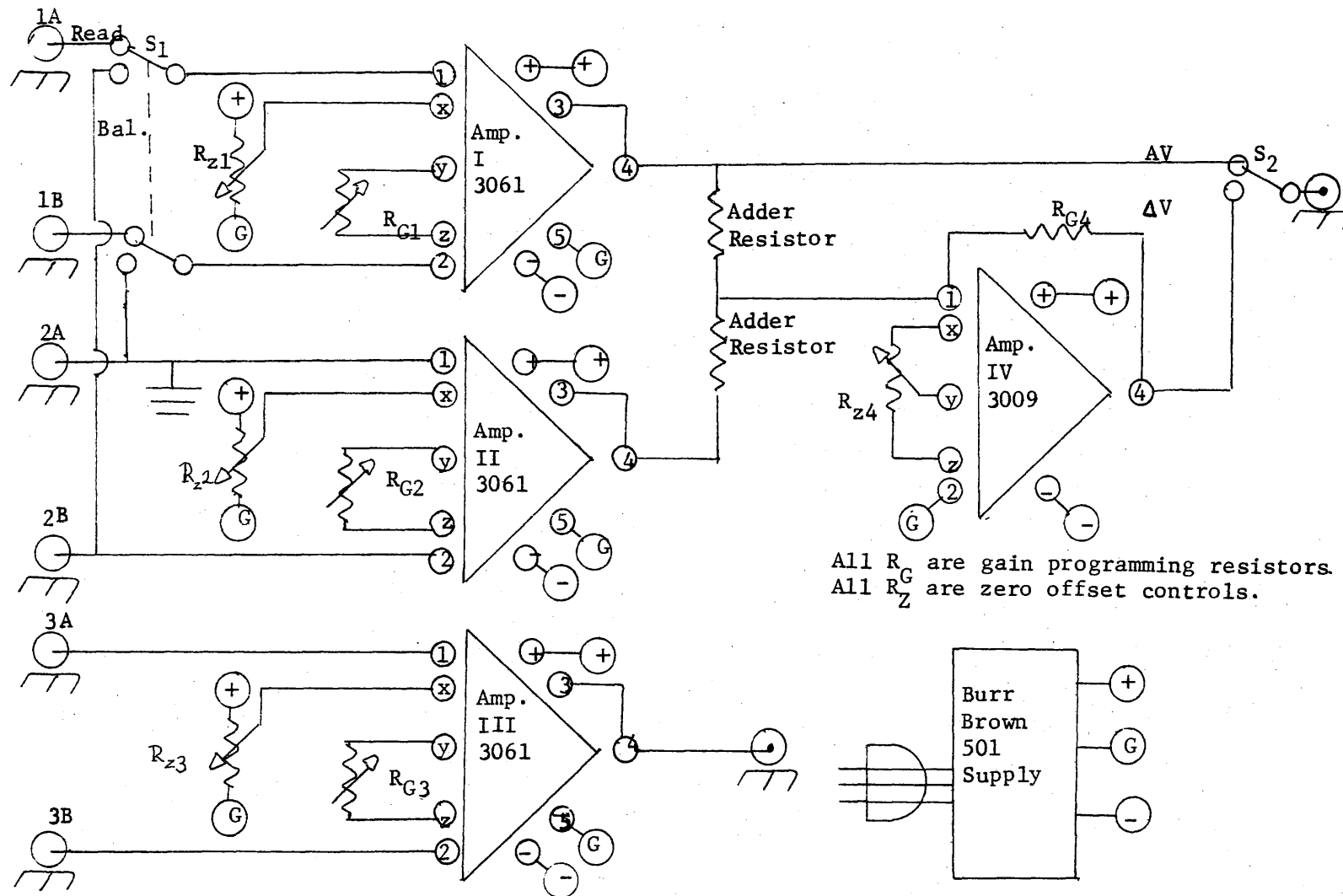


Figure 12. Circuit diagram for amplifier box.

noise. It was found that the two amplifiers matched very well at all input voltages, so when they were balanced for a high current, they were automatically balanced for the lower currents. We also noted that the amplifier balance did not usually drift much in a day of data taking, so the procedure was only repeated two or three times a day.

The second, and far more critical part of the matching was the production of "crystal balance". With the highest current which was planned for a particular run applied to the circuit, the ohmic source (R_S) was adjusted to give a "zero trace" on the oscilloscope as illustrated in Figure 13. Since the traces were far from flat, and contained quite a bit of extraneous information, (Figures 13 and 14), some qualification was selected for what was labeled a "zero trace".

It was first noticed that the trace had a steep slope from its very beginning. Since the slope disappeared below the lambda point it was felt that it came from crystal heating. To check for zero we adopted the procedure of extrapolating with a small straight edge back to $t = 0$ (Figure 14). On a "clean" trace this would have been straight forward, and indeed could have been done by eye, but the complications of the figure are greater than that. The above extrapolation was important only for readings of the non-thermal effect, because it is rather small at higher temperatures. Close to 4.2 K the thermal effect is so much larger that the question of a careful extrapolation does not arise.

To study the thermal effects, the pulses were usually long -

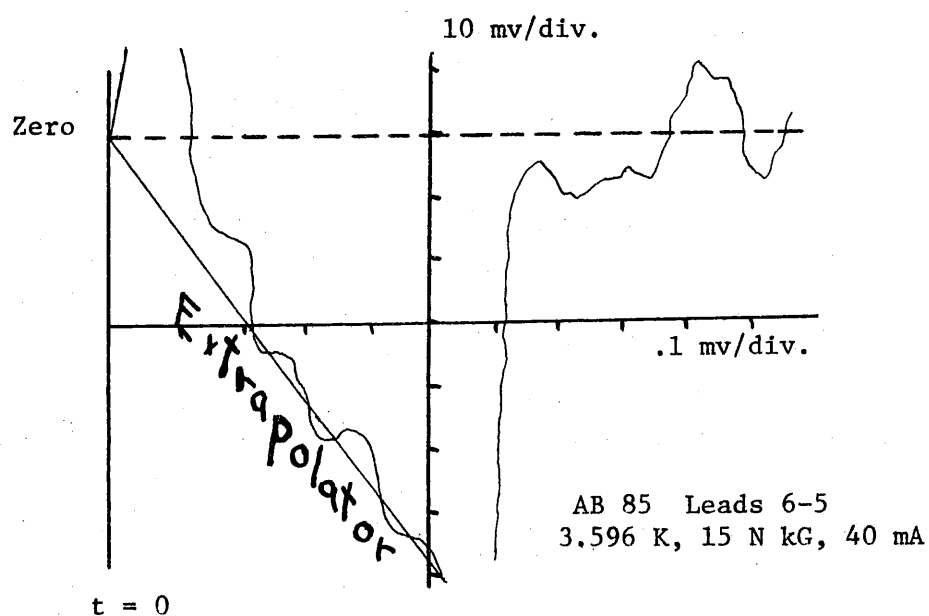


Figure 13. Typical non-thermal normalization pulse.

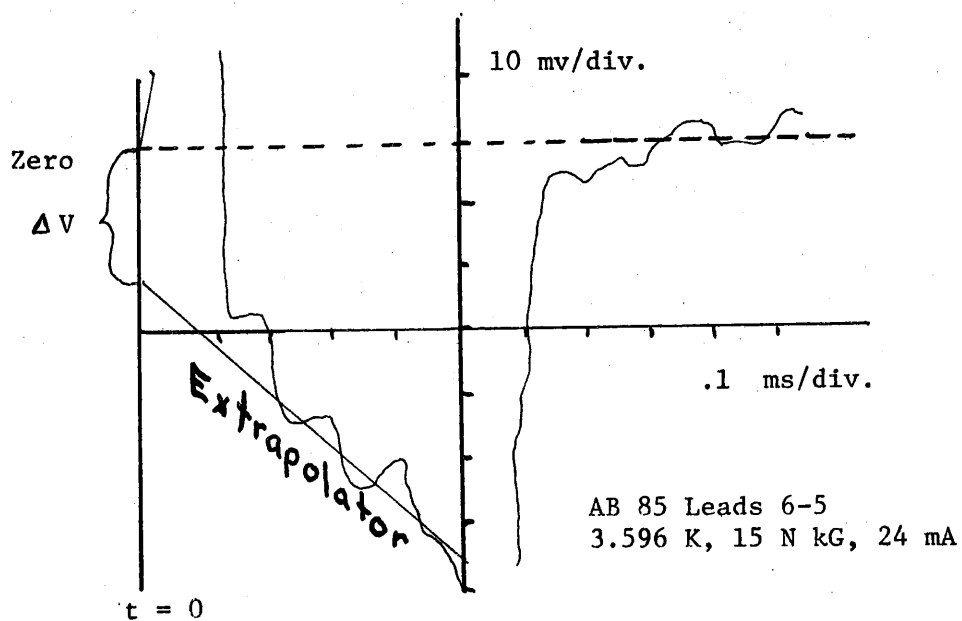


Figure 14. Typical non-thermal pulse, showing a negative ΔV , implying a non-thermal non-ohmic effect.

up to 400 milliseconds, and off times were on the order of 100 milliseconds. Occasionally, longer, manually switched pulses were used, but the techniques of reading were all the same. The non-thermal experiments used the same equipment configuration, only differing from the thermal experiments in the brevity of the pulses, and the fact that only one measurement was taken from each trace, as described later.

For each current sweep, the temperature, leads, current direction and magnetic field direction were all held fixed. The crystal balance was obtained at the highest usable current, which for Hall voltage on AB 85 was 40 mA. AB 85 magnetoresistance measurements produced voltages which saturated the amplifiers at greater currents than 16 mA. The difference voltage (ΔV) was read as the current was stepped down to 1 mA in short intervals. After the ΔV was read to get the magnitude of the non-linearity, the absolute height (ΔV) of the crystal voltage was read for each current. For a valid picture of the effect, a current sweep was needed for each direction of current and field, as discussed in the calculations.

CALCULATIONS AND RESULTS

Introduction

When the potentiometric data were plotted (Figure 15) the resistance decreased with increasing current above the lambda point, and increased below. Since both the magnetoresistance and the transverse resistance vary approximately linearly with temperature in this range, the results above the lambda point are consistent with a rise in crystal temperature with current. Below the lambda point an explanation of the results is less apparent. It is difficult to imagine that increased current could decrease the temperature, so the hypothesis was formed that some mechanism existed which was not due to thermal resistance, but had some other source. Since there was no anticipated sign for an intrinsic non-linearity the sign of such an effect could be either positive or negative. It must be admitted though, that should the non-thermal non-ohmicity be in the negative direction, the tendency would be to dismiss it as a result of some thermal process.

Before using the pulsed results, it seemed important to establish a connection with the previous potentiometric work, in the limit of long pulses. The question of the effectiveness of the balancing technique, and of the proper way for adjusting for a "crystal balance" was somewhat vague, and prompted us to apply a fair amount of time to the problem.

The results of the so-called "DC correlation" are shown in Figures 16 and 17. The error in the correlation appears to be of the same magnitude as the errors inherent in the measurement, so we felt that the differential method could be used confidently.

Thermal Results

One of the experimental goals of the pulse equipment was to separate the thermal contribution to the DC non-linearity from any intrinsic non-ohmic effect. When the existence of thermal effects was first realized, the obvious assumption was that some thermal steady state was reached above the lambda point in which heat flowed from the crystal down a thermal gradient in the bath and into the bulk helium. The resistance of the crystal then, by the time the potentiometer could measure it, would be characteristic of some temperature higher than that of the bulk bath. The plot in Figure 18 illustrates the anticipated time dependence of the pulse. Initially the temperature of the sample would be at that of the bath. If the R_S were correctly set, the ΔV trace would begin at zero, and fall because of the anticipated heating and negative dR/dT . After some time interval the trace would level off to some new steady state condition which would correlate with the previous DC data and with the resistance as measured by the potentiometer. When the pulse was turned off, the anticipated result would be an immediate drop to some low voltage which would be from the Seebeck effect, and

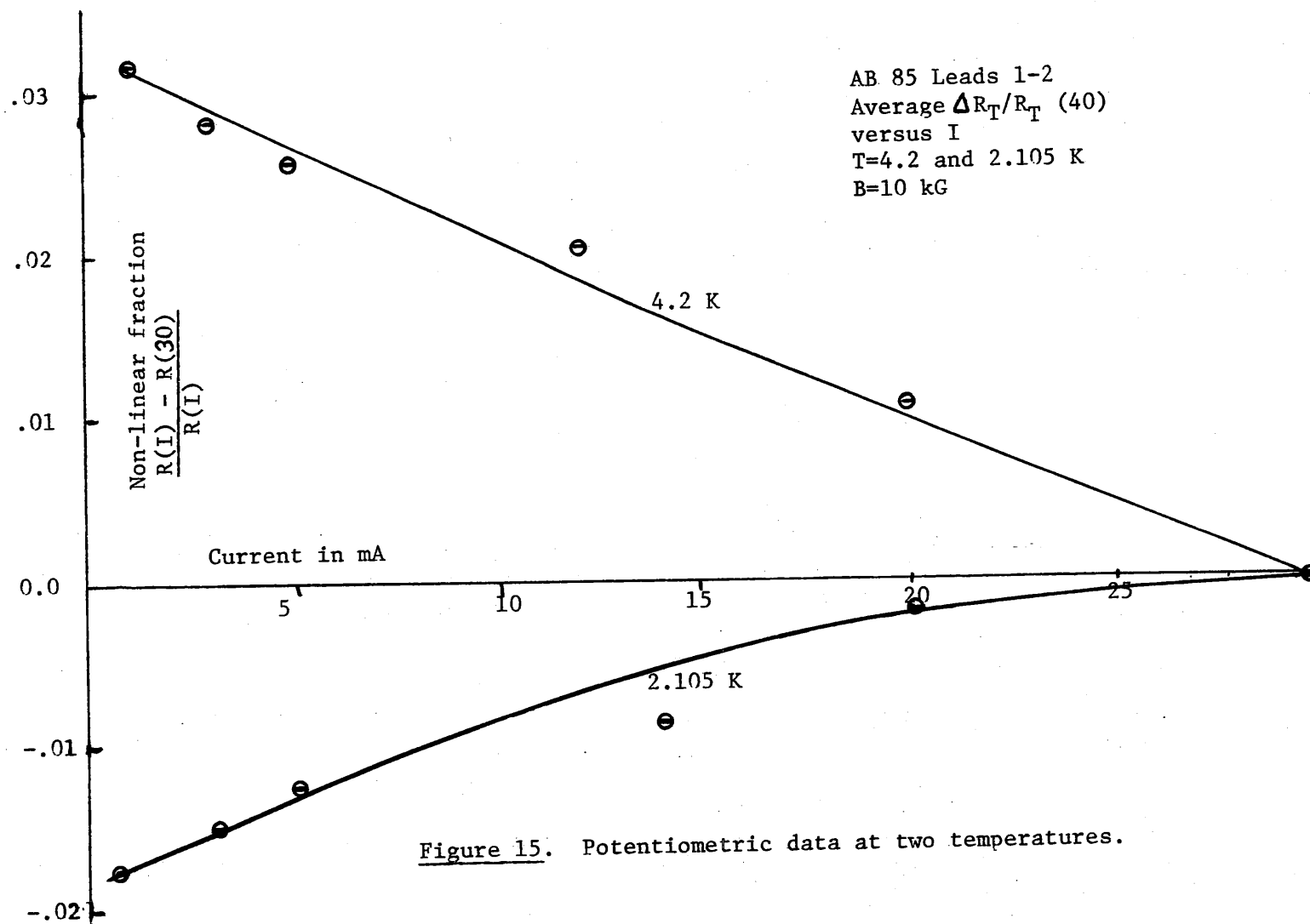


Figure 15. Potentiometric data at two temperatures.

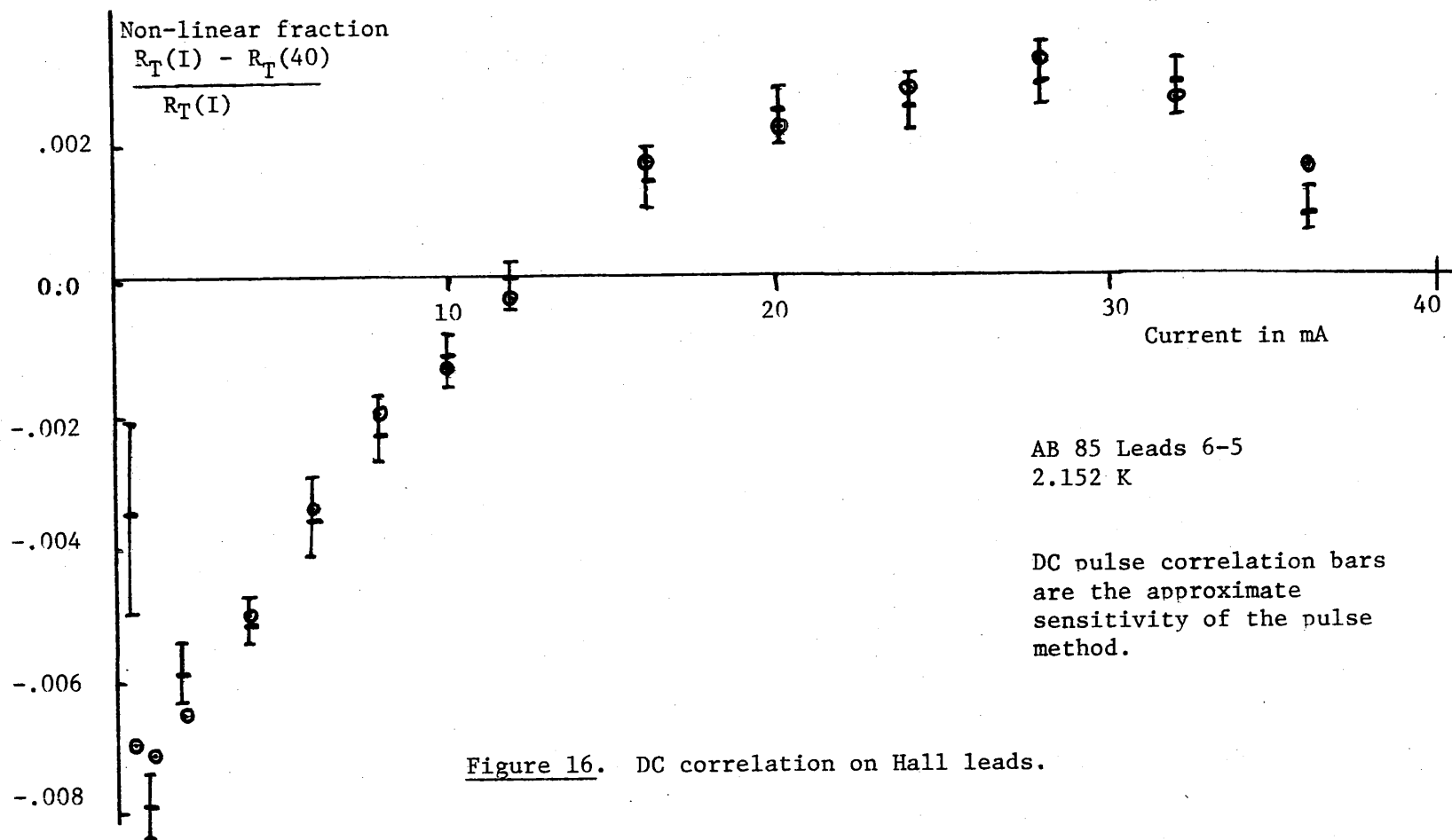


Figure 16. DC correlation on Hall leads.

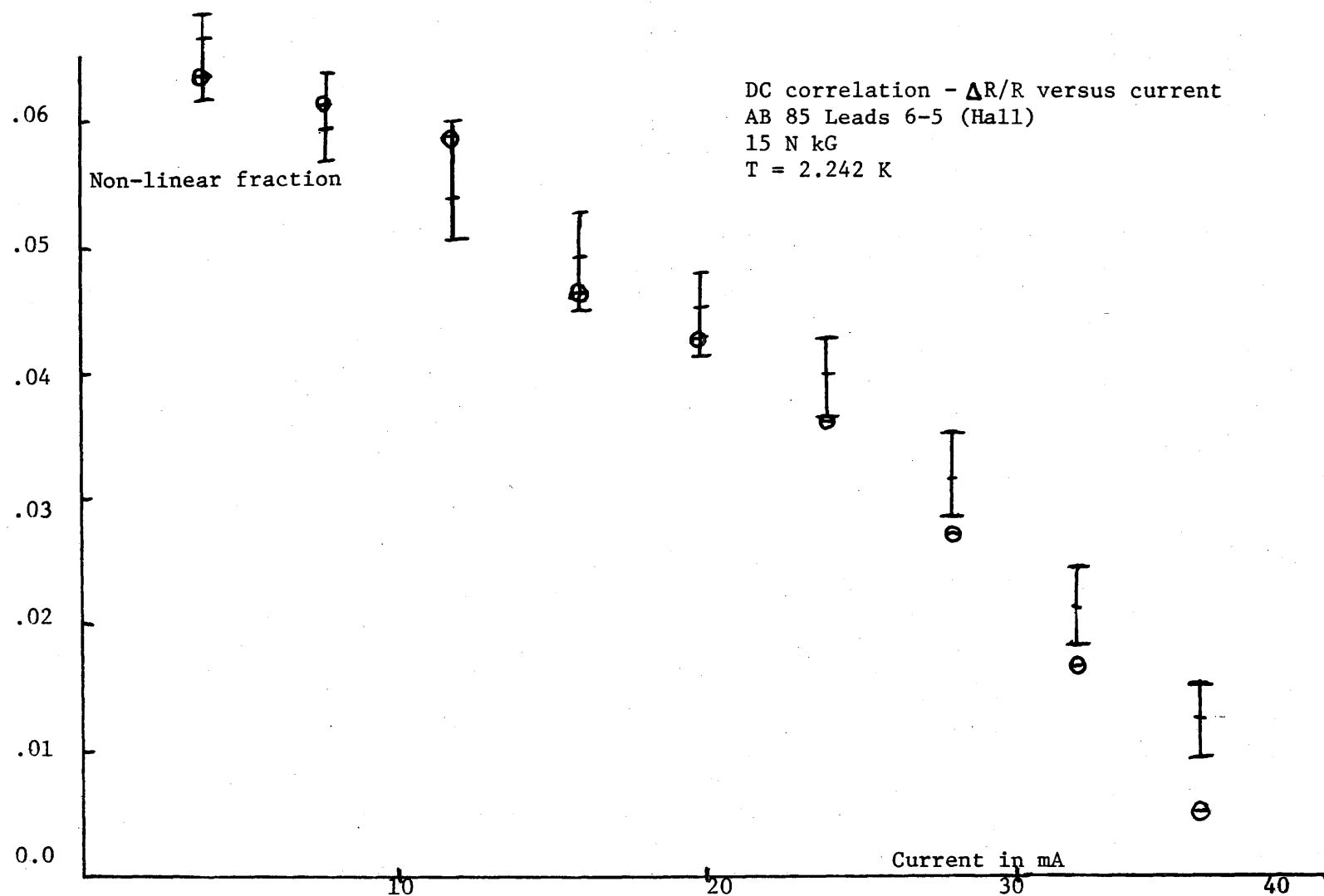


Figure 17. DC correlation (II).

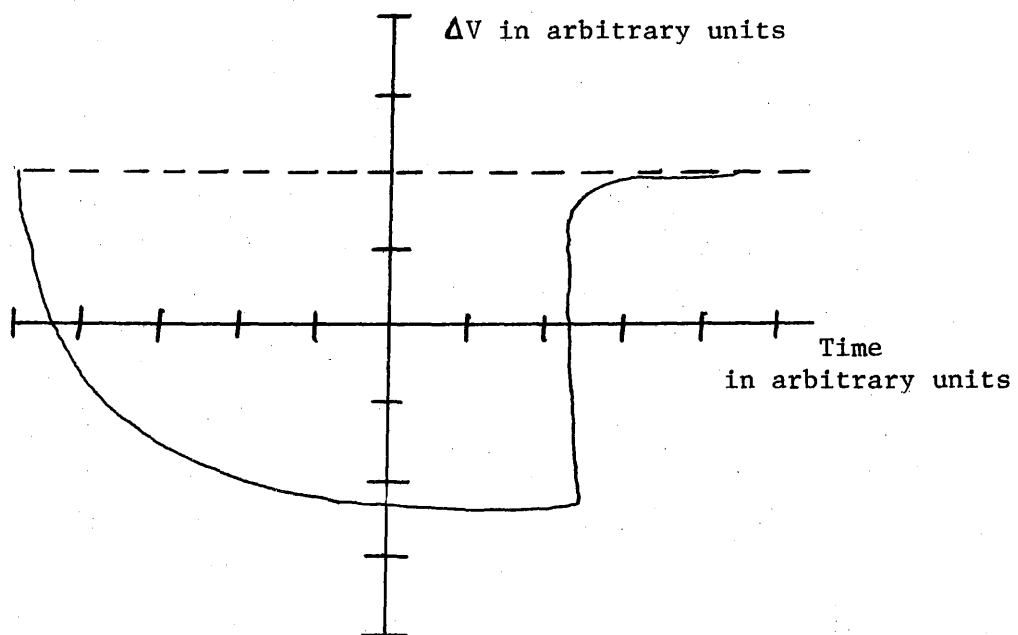


Figure 18. Anticipated time dependence of ΔV .

which would decay exponentially to the zero noted before the power was switched on.

The actual results were disturbingly different from what had been anticipated. The typical ΔV curve was as shown in Figure 19, showing a pronounced peak at about 40 ms after the onset of the pulse. The appropriate values of output voltages are given on the graph, but it must be remembered that these are amplified by a factor of 60. For this particular case the current was 40 mA and the nominal temperature 4.21 K. It may be noticed in the trace that there is an apparent lack of Seebeck voltage appearing after the pulse. This would tend to confirm that surface thermal gradients were unimportant. Of course, this is not really relevant to the calculation in Appendix A, because that calculation computes the average internal temperature which could result if the exterior were held at bath temperature. In other words, a temperature distribution, cylindrically symmetric about the longest axis of the crystal, would not produce a Seebeck voltage in our geometry.

The essence of the above argument is that the only effect which could generate so large a peak is the temperature dependence of the resistance. This would mean that the voltage trace observed follows almost exactly the time dependence of the temperature of the crystal surface, with an appropriate scale factor. Therefore, the voltage trace of Figure 19 implies that the surface of the crystal was heating rather quickly at first, and that a short time later a new heat dissipation mechanism took over to cool the crystal down to

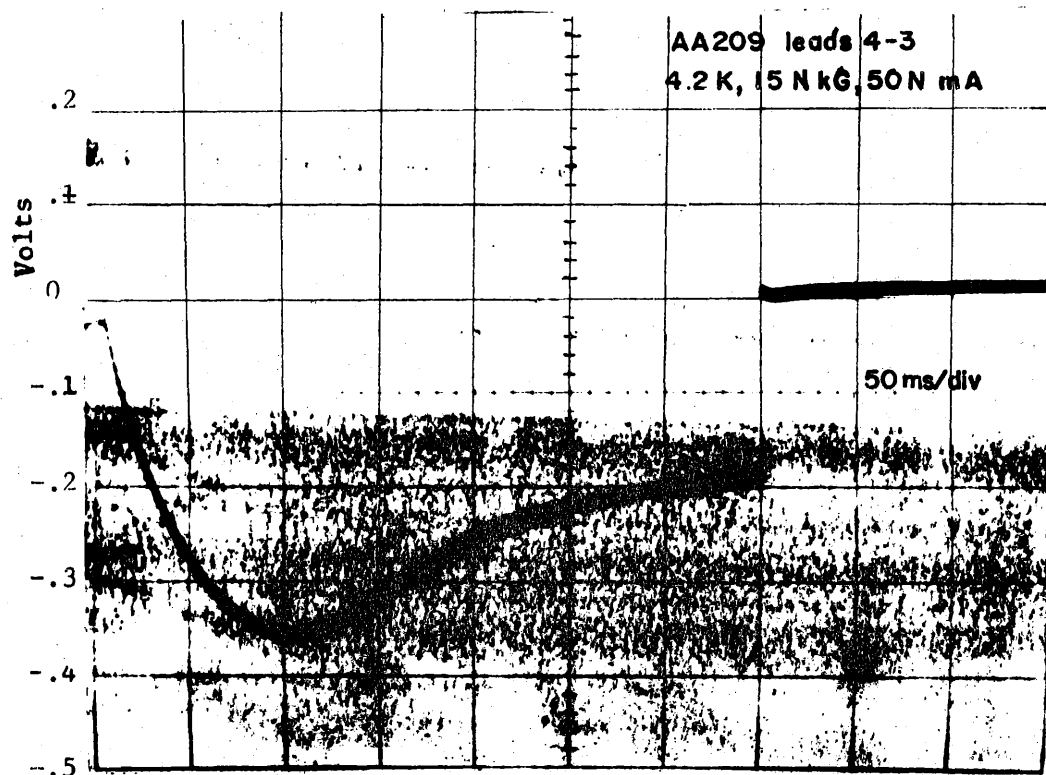


Figure 19. Typical thermal ΔV .

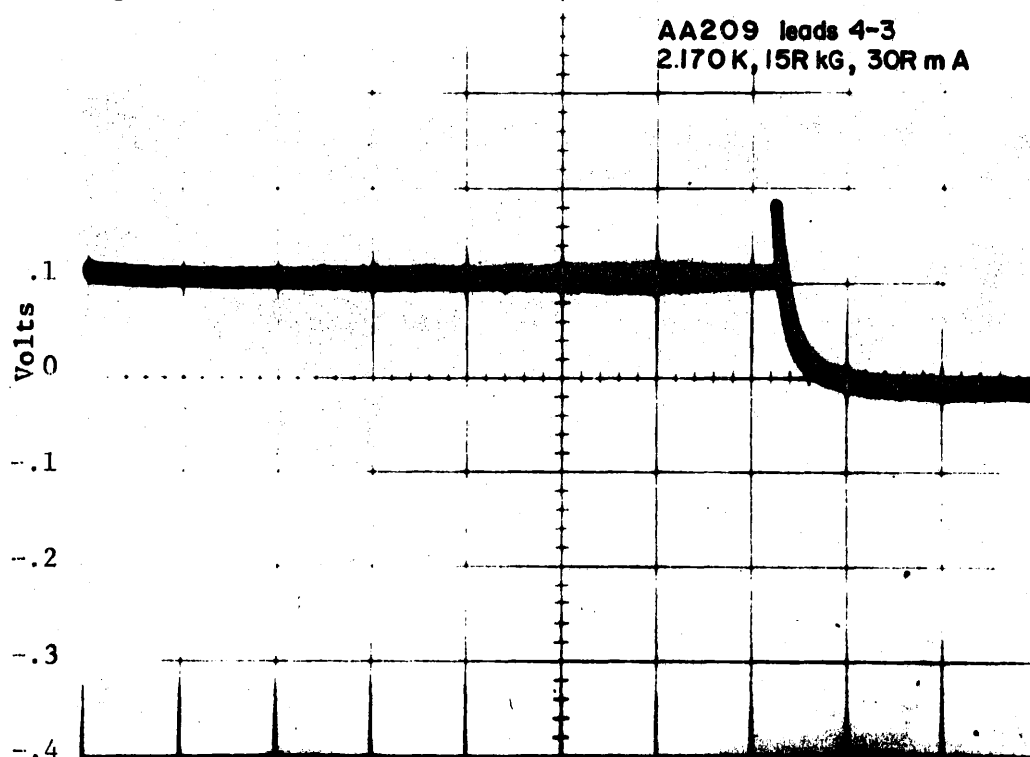


Figure 20. Typical long pulse at $T < T_{\lambda}$.

an equilibrium temperature commensurate with that suggested by the potentiometric measurements.

When this was first observed, the question immediately arose as to whether it was an artifact of our apparatus. The natural course was to pump down to the lambda transition, and observe the time dependent behavior of the resistance below the lambda point, where the superfluid properties would cool the crystal far more efficiently. When this was done, the trace changed abruptly at the lambda point, and, after a few strange gyrations became almost perfectly flat, as in Figure 20. This is what would be expected if the thermal resistance were all in the liquid, as had been suggested previously by the DC results. This even seemed to eliminate the thermal boundary resistance (Kapitza Resistance (9)) as a source of heating, since there is no reason to suspect that it would be discontinuous across the lambda point.

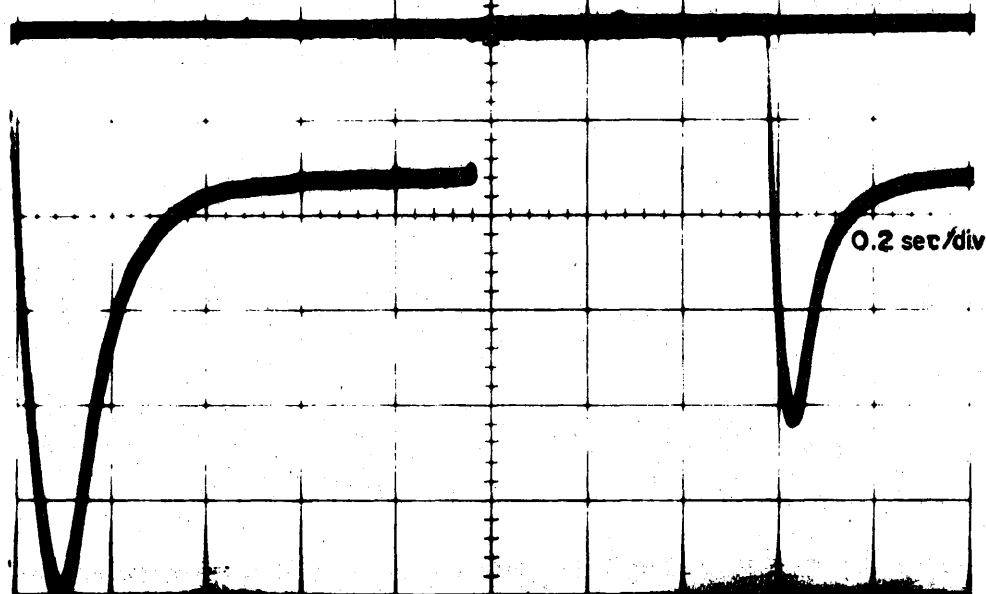
An interesting feature of the second more efficient mode of heat conduction is its long remanence. It was noted that the first time a pulse was sent into the crystal, after a long rest, the change in temperature which resulted was about twice or three times that of subsequent pulses. This result was dubbed the "virgin pulse effect" and two different displays of it are shown in Figure 21. The temperature dependence of this effect was measured and it seems to be similar to that of the peak. It was concluded from this effect that the cooling mechanism which produces the upturn of the peak has a duration much longer than the warming mechanism which initiates it. The peaks increase in magnitude as the rest time

increases with a half-time of approximately 30 seconds.

Several mechanisms have been proposed to account for this peak. One of the first was the onset of film boiling, a mode of heat conduction in which the solid surface is insulated by a continuous film of vapor, and which has a relaxation time perhaps on the order of ours. This explanation is inappropriate for two reasons. First, the threshold heat flux for film boiling is about 500 mW per cm^2 (10) at room pressure, and our heat input was never so large. Assuming a magnetoresistance between two leads of about $30\ \Omega$ and the longitudinal separation to be about .7mm, the power output for the geometry of AB 85 at the maximum current of 40 mA was approximately $50\ \text{mW}/\text{cm}^2$, about a tenth of that needed. The more basic objection is that the onset of film boiling would cause a rapid and violent temperature rise rather than the cooling suggested by our results.

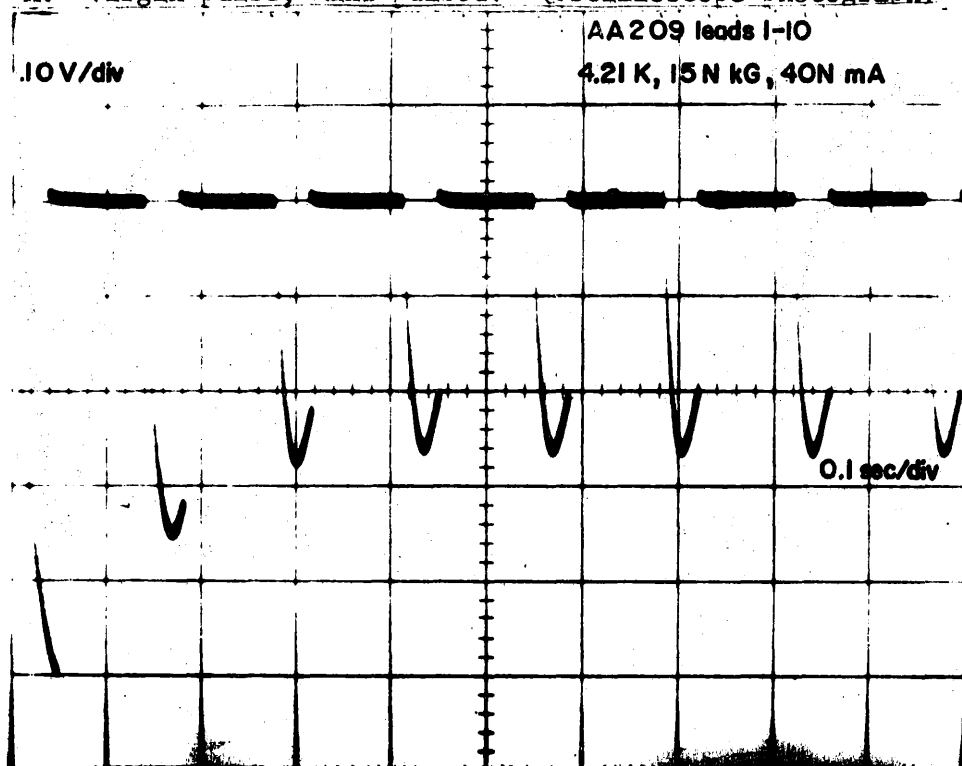
The Kapitza resistance, as mentioned above, has been proposed several times as a mechanism. However, it is difficult to explain the striking disappearance of any recognizable heating below the lambda point, when just above the lambda point the effect is so obvious. A second objection to the Kapitza resistance hypothesis is that we have not observed the usual strong temperature dependence (11). In the source cited, Kapitza resistances have been found to be proportional to $T^{-\chi}$ where χ has values from 2.5 to 3.2, but no such high exponent was revealed by our data. The final objection is that even though the Kapitza resistance is not theoretically understood, there seems no reason to imagine that it could be time dependent.

0.1 V/div

AA209 leads 4-3
4.21 K, 15N kG, 50N mA

A. Virgin pulse, hand pulsed. (Oscilloscope photograph)

.10 V/div

AA209 leads 1-10
4.21 K, 15N kG, 40N mA

B. Virgin pulse, machine pulsed. (Oscilloscope photograph)

Figure 21.

Perhaps a sidelight might be mentioned in connection with the Kapitza resistance. At the time when that seemed an attractive hypothesis, Mr. Charles Hartley (12) suggested that the discontinuity at the lambda transition might be due to a change in effective surface area instead of a discontinuity in the phenomenon itself. His reasoning was based on the fact that bismuth crystals have been thought to have fine cracks in their surface. If a large percentage of cracks were too fine for the normal fluid to penetrate, but coarse enough to allow the superfluid to enter, the area available to heat dissipation might increase enough during the lambda transition to produce the flattening of the thermal pulse.

Hartley's idea still does not seem to produce a time dependence for the peak in the normal fluid, nor does it advance any arguments for the lack of strong temperature dependence. Therefore, it appears that Kapitza resistance must still be dismissed on these grounds, but the possibility remains that Hartley's mechanism exists to enhance thermal conduction below the lambda point.

Still another hypothesis for explaining the peak is the appearance of a boundary layer of warmed liquid around the crystal. It was thought that perhaps after the layer had had a short time to warm, its density would change enough to initiate convection, and the continued convection currents would constitute the more efficient cooling mechanism indicated by the time dependence of the temperature. When an attempt was made to calculate the time needed to initiate a laminar flow, it was found that the necessary time was at least an order of magnitude too long, so it was felt that laminar

flow could not be an adequate mechanism.

In connection with these hydrodynamic mechanisms, Mr. Arnold Moodenbaugh made some calculations to investigate the possibility that an initial laminar flow changing to a turbulent flow would perhaps produce more efficient cooling. Making rather drastic assumptions he found that the minimum time was about 5 seconds, which is also far too long.

The only model which does not lead to obvious contradictions is the hypothesis that a small superheating takes place in the layer of helium next to the crystal during the first prepeak stage of the trace. As the superheating begins to induce greatly enhanced bubbling at nucleation sites on the crystal, it cools back down to a steady state temperature due to the dissipation of the Joule heat in vaporizing the helium to form the bubbles. In addition to explaining the abrupt change in trace shape at the lambda point this mechanism accounts for the fact that the crystal trace seems to be smoother before the peak than after. Since during the superheating phase very little bubbling is going on at the crystal surface, the environment is relatively calm and the two potential leads are fairly still. After nucleation begins at the liquid-crystal interface, the potential leads are constantly being jostled by the bubbles, and, as pointed out in Appendix C (coherent noise calculations) the smallest motion of the tiny lead wires would be noted on the oscilloscope.

The fact that the peak is only slightly dependent on temperature

is also explained by this model. At 4.2 K the peak is pronounced at currents of 40 mA and disappears by about 10 mA (Figure 22), but as the temperature is lowered, the peak disappears at higher and higher currents. The explanation which seems plausible is that at the lower temperatures the continual boiling is so much more violent that the superheating cannot occur.

While many of the salient characteristics of the data may be explained from this viewpoint, an experiment done to test it was inconclusive. When a set of carbon resistors was substituted for the crystal, there was no sign of the peak. The result was more like our anticipated behavior for the bismuth crystal (Figure 18). Furthermore, the carbon resistors did not show the complete wipe off that the bismuth did when the lambda point was passed. Consequently, it was felt that the carbon behavior was due to a temperature increase within the bulk material rather than being a surface effect. (In passing it should be noted that there was no non-thermal effect, either.)

The interplay between all of the thermal effects could be observed at the lambda transition as is displayed in Figure 23. When long pulses were used, the gyrations of the trace were very complex, and an explanation was not at all apparent. The sequence is as shown for a monotonic cooling, though the pictures are not necessarily separated by constant temperature intervals. Reversibility was the first feature of the sequence to be observed. It was also found that by careful manipulation of the pumping speed the trace could be held at one particular configuration for a rather

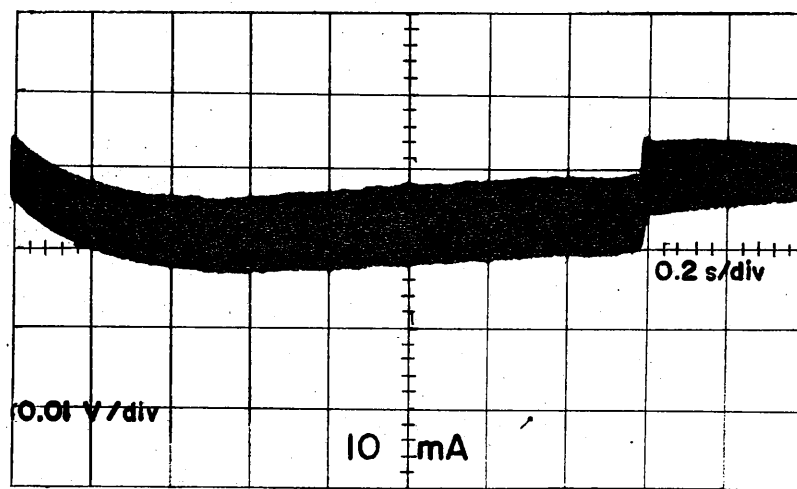
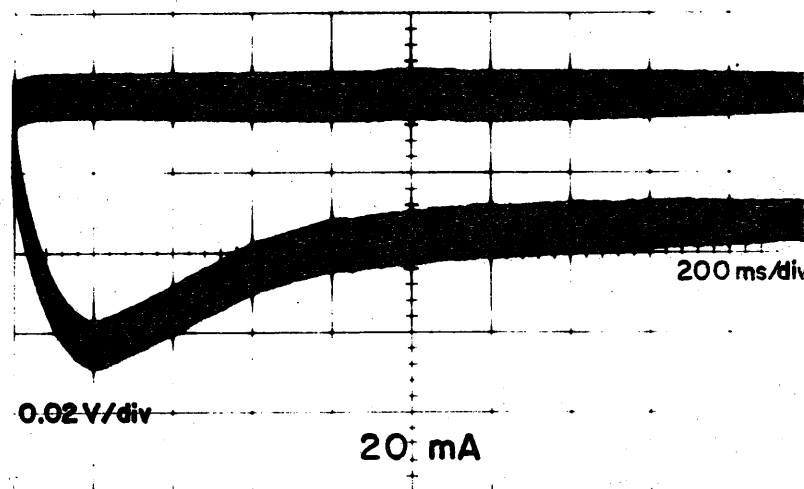
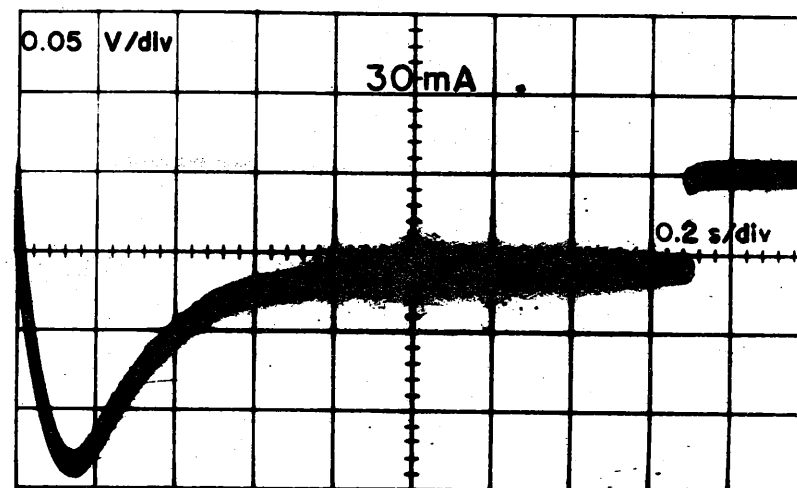
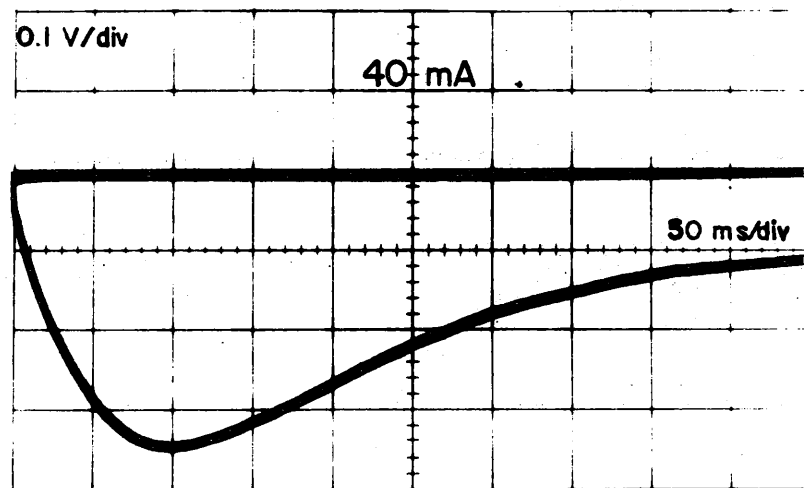


Figure 22. Current dependence of peak. AA 209 Leads 4-3, 4.2 K, 15 N kG, Curr = N

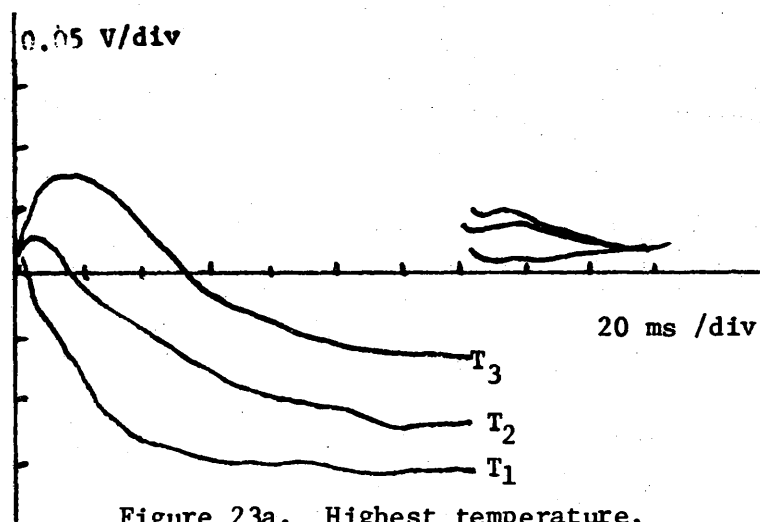


Figure 23a. Highest temperature.

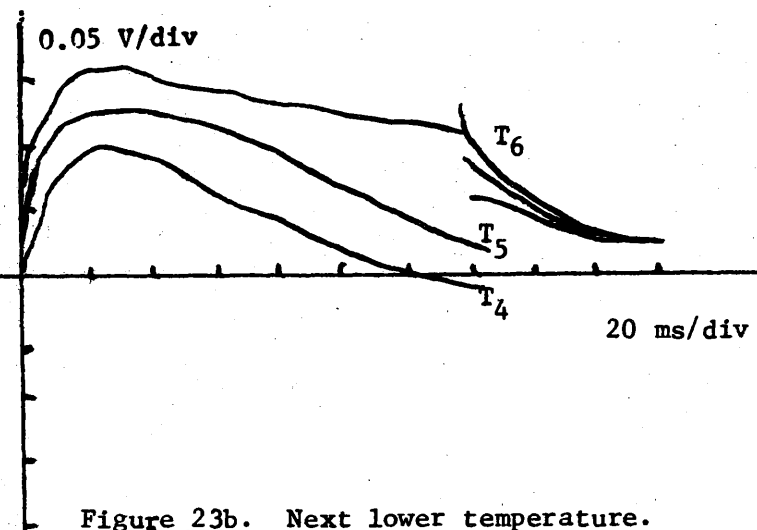


Figure 23b. Next lower temperature.

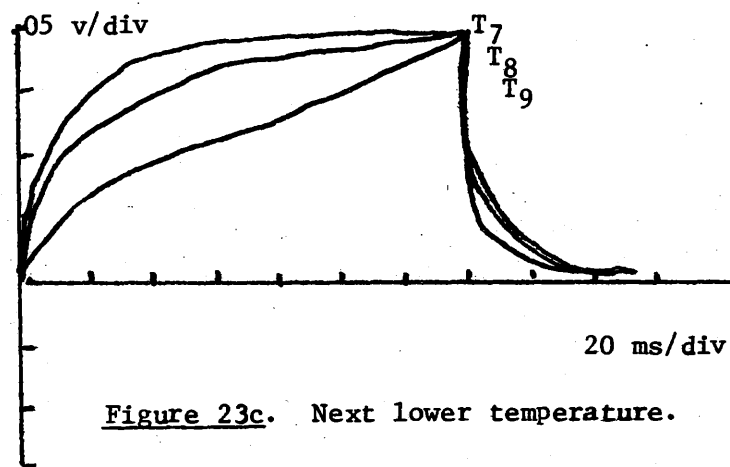


Figure 23c. Next lower temperature.

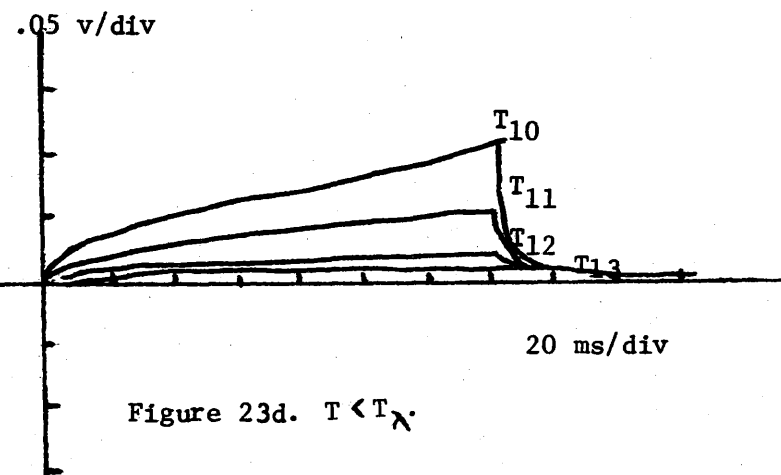


Figure 23d. $T < T_N$.

Figure 23. The lambda sequence monotonically cooling for AA 209, leads 9-8, with $B = 15 \text{ N kG}$, and $I = 40 \text{ N mA}$.

extended time. It was further noted that for lower currents the effect was far less dramatic, although still present.

The only conclusion which seemed reasonable for this rather complex effect was a model in which the lambda transition was not limited to one pressure but occurred over a range of pressures. Our attention was directed to a paper by Ahlers (13) in which the effect of the gravitational field on the lambda transition was discussed. It was his conclusion that a boundary exists between the superfluid and normal phases of liquid helium in the presence of a gravitational field. Because of the negative slope of the lambda line on a pressure-temperature plot the normal fluid would be on the bottom where the pressure was greatest and the superfluid would extend from the boundary to the surface. Thus even if the bath were at the same temperature throughout, the thermal conductivity would be vastly different on the two sides of the boundary. Of course the normal part of the bath would not be all at one temperature, because of the pressure gradient due to the helium density.

Therefore, since the temperature gradient in the body of the crystal was negligible when a pulse was sent into the crystal, the discontinuity in the thermal conductivity manifested itself in a discontinuity in surface temperature in the crystal. Since any temperature gradient along the surface would meet the requirements for a copper-bismuth thermocouple, the discontinuity could easily be registered on our equipment.

The general outline seems clear, but the specific details are not so easy to describe. There was some question as to the distance over which the temperature distribution was appreciably non-uniform. Ahlers points out that classically one obtains for the change in pressure, ΔP , two points in a fluid vertically separated by ΔH , $\Delta P = g \Delta (\rho H)$, where ρ is the fluid density and g is the acceleration due to gravity. For a small change in lambda temperature, T_λ , and pressure, we may assume ρ and $\frac{\partial T_\lambda}{\partial P}$ to be constant and $\frac{\partial T_\lambda}{\partial H} = \frac{\partial T_\lambda}{\partial P} \frac{\partial P}{\partial H} = \rho g \frac{\partial T_\lambda}{\partial P}$.

Approximately, $\Delta T_\lambda = \rho g \frac{\partial T_\lambda}{\partial P} \bigg|_{T_\lambda} \Delta H$ and we may define a constant a such that $\Delta T_\lambda \equiv a \Delta H$. Ahlers calculates a to be $(1.273 \pm .003) \times 10^{-6}$ K/cm. This indicates that if the discontinuity had to be localized within two leads about .8 cm apart to see the lambda sequence, control would be needed to within less than a micro-degree. This is two orders of magnitude below the sensitivity of our equipment. It might be possible, though, that the infinite thermal conductivity of the helium II could act as a heat sink for the whole crystal. Since the thermal conductivity along the crystal is so much better than that of the normal bath, the Joule heat generated in the crystal would be dissipated through the end rather than through the faces. Therefore the temperature range of the lambda sequence would be increased by an order of magnitude because the total length of the crystal is about 10 times the lead separation.

It was somewhat more difficult to rationalize similar effects when they appeared on the transverse lead pairs. The mechanism

hypothesized was that the Ettingshausen effect tipped the isothermal surfaces so that the transverse leads were not at the same temperature. However, some experiments done to verify this mechanism by correlating the observations to the magnetic field and current direction were inconclusive.

Non-thermal Non-linearity

After some survey work on the many aspects of the pulsed signal, it was decided to exert most of the effort on quantitative study of the hypothesized intrinsic, that is, non-thermal non-ohmic effect. It was felt that continuity across the lambda point would be the positive proof of an intrinsic non-ohmicity, and thus the temperature dependence would be a prime factor in deciding on the question of its existence. Before discussing the actual data, perhaps some of the technique for interpretation should be reviewed.

As described in the section titled "Procedure", the trace (Figures 13 and 14) was very cluttered with spurious information as viewed on the scope. Perhaps the most difficult problems were the spikes at either end of the pulse. Due to the wide differences in the length of the input leads to the amplifiers 1 and 2, there was some mismatch in the input capacitances, and when the ohmic signal was subtracted from the crystal voltage, the mismatched component did not subtract out. The procedure followed was to

disregard these spikes, and accept only the data from the later part of the extrapolation (Figure 14).

Interpretation of the pulse was also complicated by a large white noise background, which was present in the crystal signal at all times. Several attempts were made to eliminate this, but most were less than successful. It was found, though, that if the nitrogen were cooled by pumping on it, repressurized, and allowed to warm without boiling, the noise amplitude diminished considerably. It changed from a value of about 6 millivolts to approximately .1 millivolt, as referred to the final output at a total gain of 60. Apparently the nitrogen bubbles jostled the inner dewar, and, as discussed more fully below, the smallest disturbance would be seen in our equipment.

However, a more irritating fact was that there was a large component (final output value of approximately 2 mV) of "noise" which was coherent with the pulse, and which, moreover, had a distinct frequency in the range from 500 to 1000 Hz depending upon the particular leads being used. The hypothesis which was suggested was that when the current pulse passes through the crystal located in the strong magnetic field, the resulting Lorentz force moves the crystal slightly. The motion of the crystal set up vibrations of the potential leads with respect to the magnetic field. If the number of flux lines within the loop formed by the potential leads and their connection through the crystal were changed, a voltage would be generated in the loop. Since the inputs to the amplifier have a very high impedance,

very little current would need to flow to be seen on the output. This hypothesis is supported by the observation that the noise decreased in amplitude when the leads were glued down more carefully. Finally, a calculation was made (Appendix C) which implied that motion of less than the diameter of a wire was sufficient to excite the observed voltages. Since no easy solution for this problem suggested itself the only apparent procedure was to perform an optical "least-squares" analysis of the acceptable part of the trace (Figure 13 and 14) and extrapolate that to zero time. The voltage zero was defined by a similar optical least squares analysis of the "off" part of the trace, and the high current balance was referred to this zero.

The unfortunate feature of such an extrapolation is that it introduces a strong element of uncertainty. Because the attempt was consciously made to avoid that part of the pulse which was closest to the point toward which the extrapolation was aimed, a small variation in weighting the points which were used would cause a large fluctuation in the reading. The possibility, then was great for operator prejudice to influence the results. The fortunate part of the procedure of using changing current intervals, and ratios of two measurements, is that the operator had little idea of how to prejudice himself. Furthermore, the operator was aware of the possibility and attempted to avoid it.

Misalignment of leads. A question which is crucial to resolve is that which arises when Hall leads are not directly transverse from each other. Since the magnetoresistance was

about 3.8 ohms per millimeter, and the "transverse resistance" totaled only about 3.6 ohms, the slight misalignments inherent in attaching leads tended to be very obvious in the transverse data.

In the absence of a magnetic field the equipotential surfaces are projected as lines which are reasonably straight and horizontal in the experimental area, as in Figure 24a. The resistance of the crystal separates the lines, and the lack of a transverse voltage is illustrated by the fact that they are perpendicular to the current. When the magnetic field is applied, the situation is changed to Figure 24b. The Hall voltage appears as a tipping of the equipotentials. The angle indicated as θ_H in the diagram is called the Hall angle and may be calculated as $\theta_H = \arctan \left(\frac{E_T}{E_L} \right)$. When the magnetic field reverses, (Figure 24c), the equipotentials have their slope multiplied by -1. The case of the directly transverse leads (a-b in these two figures) is clear; the voltage between the two changes sign. In the case of leads a-c, however, only part of the voltage reverses. Thus if V_{TN} is the Transverse voltage in the Normal field, $V_{TN} = V_{||} + V_H$. In the Reverse field $V_{TR} = -V_H - V_{||}$, and, solving for V_H ,

$$V_H = \frac{V_{TN} - V_{TR}}{2} .$$

Finally, consider leads a-d in the same pair of figures. The voltage between these no longer even reverses, but the analysis above still holds, and $V_H = \frac{V_{TN} - V_{TR}}{2}$. The reason for mentioning this last case is that on AB 85 there is a set of leads with this

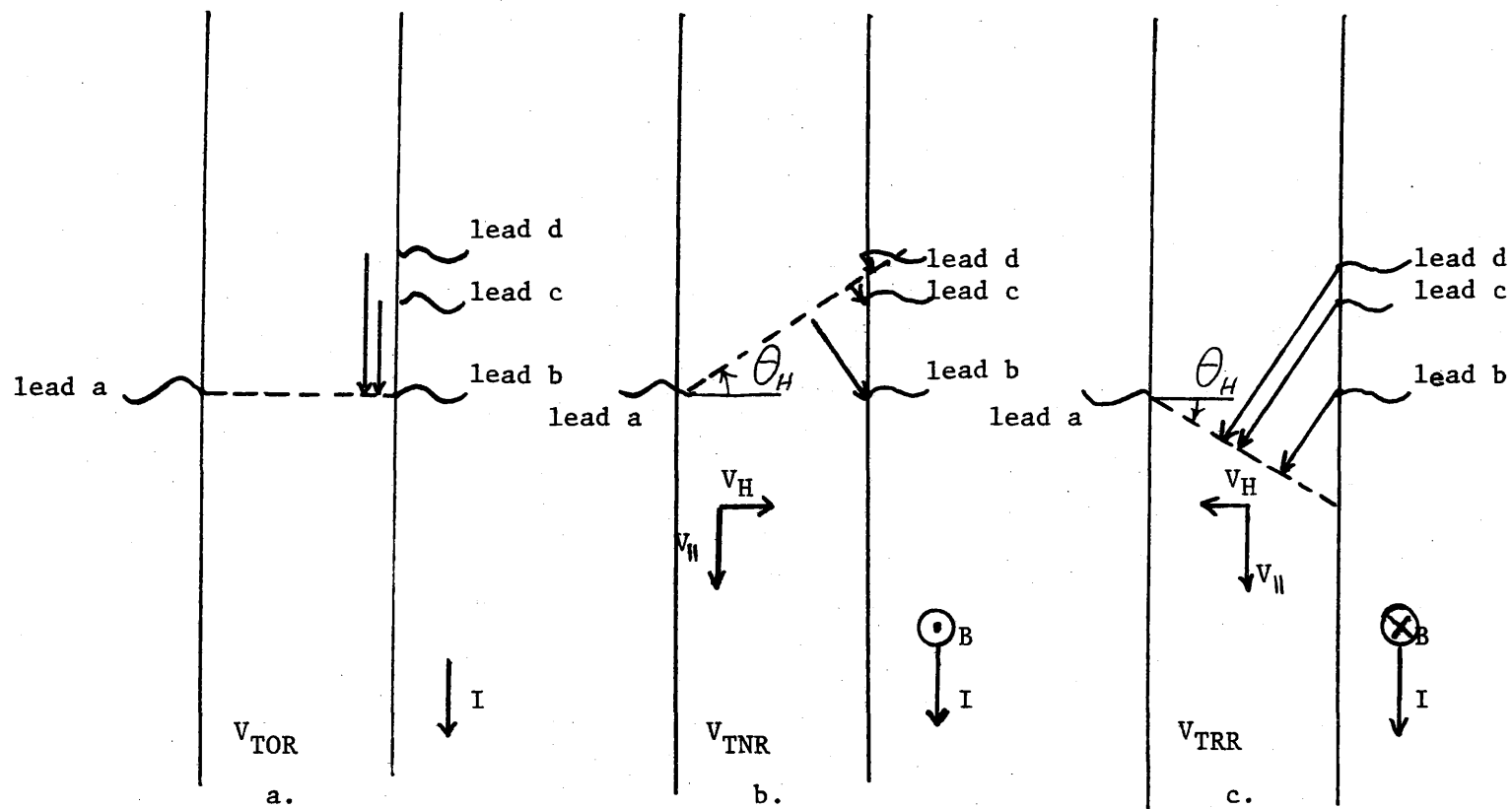


Figure 24. Effect on the Hall voltage of various degrees of misalignment.

difficulty, of which more will be said.

The compensation for misalignment on the transverse leads was the most important compensation technique. It turned out to be necessary to average the two current directions also, as shown in a sample data curve (Figure 25), since either current direction, taken alone produces a curve different from the average. The only suitable procedure was to average the data obtained at a specific current from the four possible combinations of directions of the current and field.

Experimental Results and Interpretations. Since the apparent non-thermal effect had been observed to be largest on the Hall lead pairs, most of the search for it concentrated on these pairs. On crystal AB 85, there were two pairs of usable transverse leads, as shown in Figure 5. On these two pairs the observed non-linearity had a similar magnitude after averaging to eliminate the misalignment effects. Typical data obtained from a set of four current sweeps on each lead at a common temperature are presented in Figures 25 and 26. For leads 4-3, it may be surprising to note that for the RR combination some of the non-linearities in the resistance are apparently greater than the resistance. This was equally startling to the experimenters, who spent considerable time in discussion before coming to a model which seems to fit reasonably well.

Experimentally, on leads 4 and 3 there are two peculiar results. First, the crystal voltages are very small for the Reverse orientation of the magnetic field. In addition, the crystal voltage does

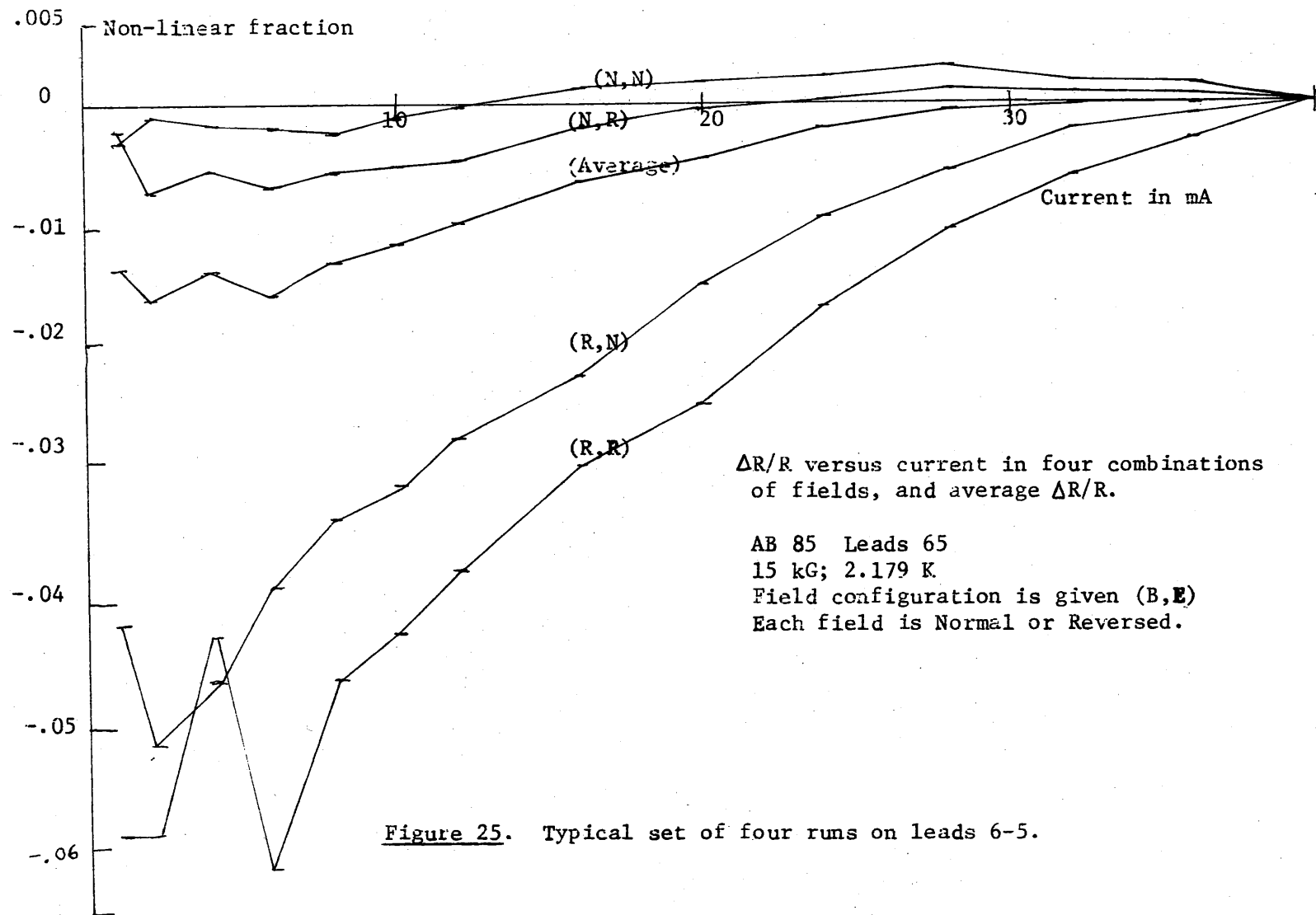
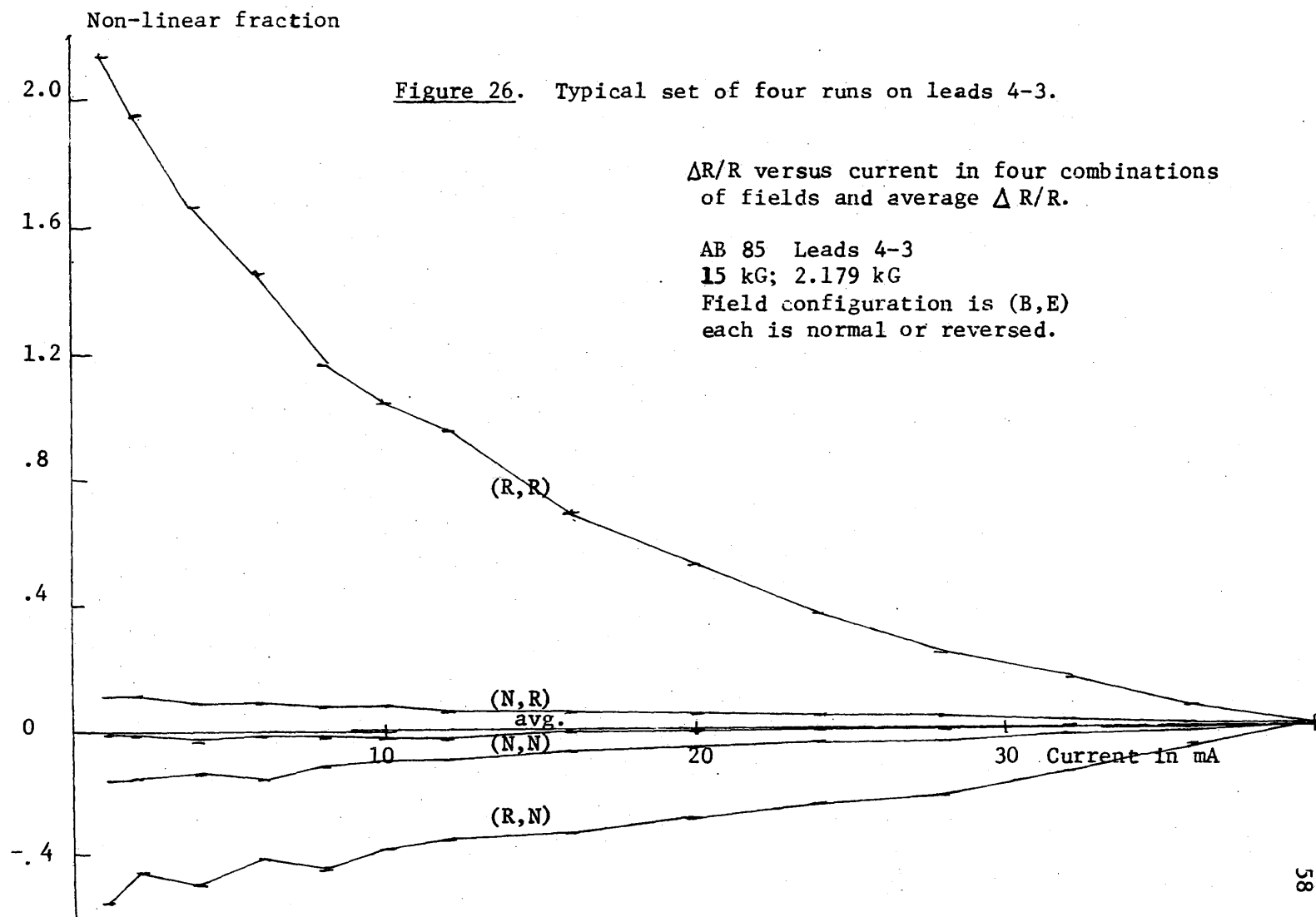


Figure 25. Typical set of four runs on leads 6-5.



not change sign for Reverse current when the magnetic field is reversed, but does when the current is Normal. The most conclusive indication of the non-reversal of AV is the fact that the "crystal balance" does not require the leads to be reversed. It is interesting that even though the AV's are small for Reverse magnetic field, the ΔV 's are of a normal size. Therefore, the normal measure of non-linearity, $\Delta R/R$, becomes very large for this magnetic field direction (Figure 26). The explanation adopted is diagrammed in Figure 27. The misalignment of leads 4-3 was assumed to be so large that the equipotential from lead 3 in the Reverse magnetic field, Reverse current, combination is on the same side of lead 4 as the equipotential for Normal magnetic field.

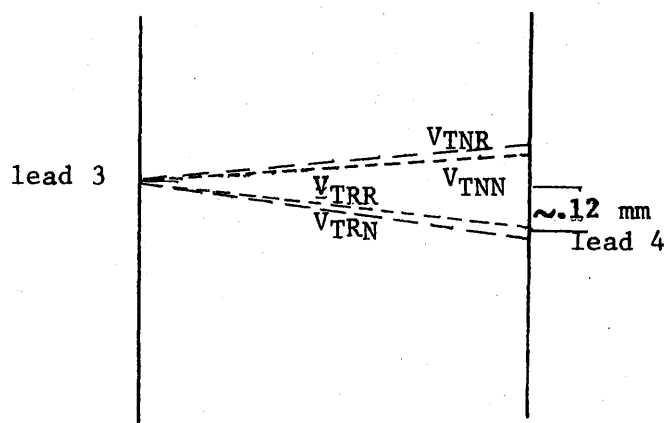


Figure 27. Diagram for model of leads 4-3, AB 85.

This would be the reason that the transverse voltage for Reverse magnetic field and Reverse current, V_{TRR} , has the same sign as V_{TNR} . By coincidence, lead 4 falls between the RR equipotential and the RN equipotential, so V_{TRN} is of the opposite sign to V_{TNN} .

After the explanation had been proposed, the crystal was observed with a traveling microscope and the leads were seen to be misaligned by $(.12 \pm .03)$ mm. This unusually direct measurement implies that the Hall angle is about $\hat{\Gamma} \ 26' \pm 20'$ of arc. This compares fairly well with the value of $52'$ calculated from $\theta_H = \frac{E_H}{E_L}$.

This source of confusion turned out to be rather fortuitous, because it allowed display of the non-thermal effect rather graphically. In the equipotential plane representation, any non-ohmic effect is seen as a rotation of the equipotential planes in the plane of the magnetic field. It might be noted, however, that should the non-ohmic effects in the longitudinal direction be the same percentage and sign as that in the transverse direction, the rotation would be zero. The data we have on the magnetoresistive leads does not bear this condition out, since the non-thermal effect in the longitudinal pairs is at least an order of magnitude smaller than the transverse intrinsic non-linearity.

However, the experimental results show a reversal in sign of ΔV during a current sweep in the RR combination of fields at several temperatures as in Figure 28. This seems so positive a demonstration of the existence of a rotation as a function of current that it should be included in this discussion though the contribution to the quantitative understanding of the effect from these rather unusual results was really no greater than from any other direction combination.

The current dependence of the two lead pairs is shown in Figures 29 and 30 where an intrinsic non-ohmic effect is clearly

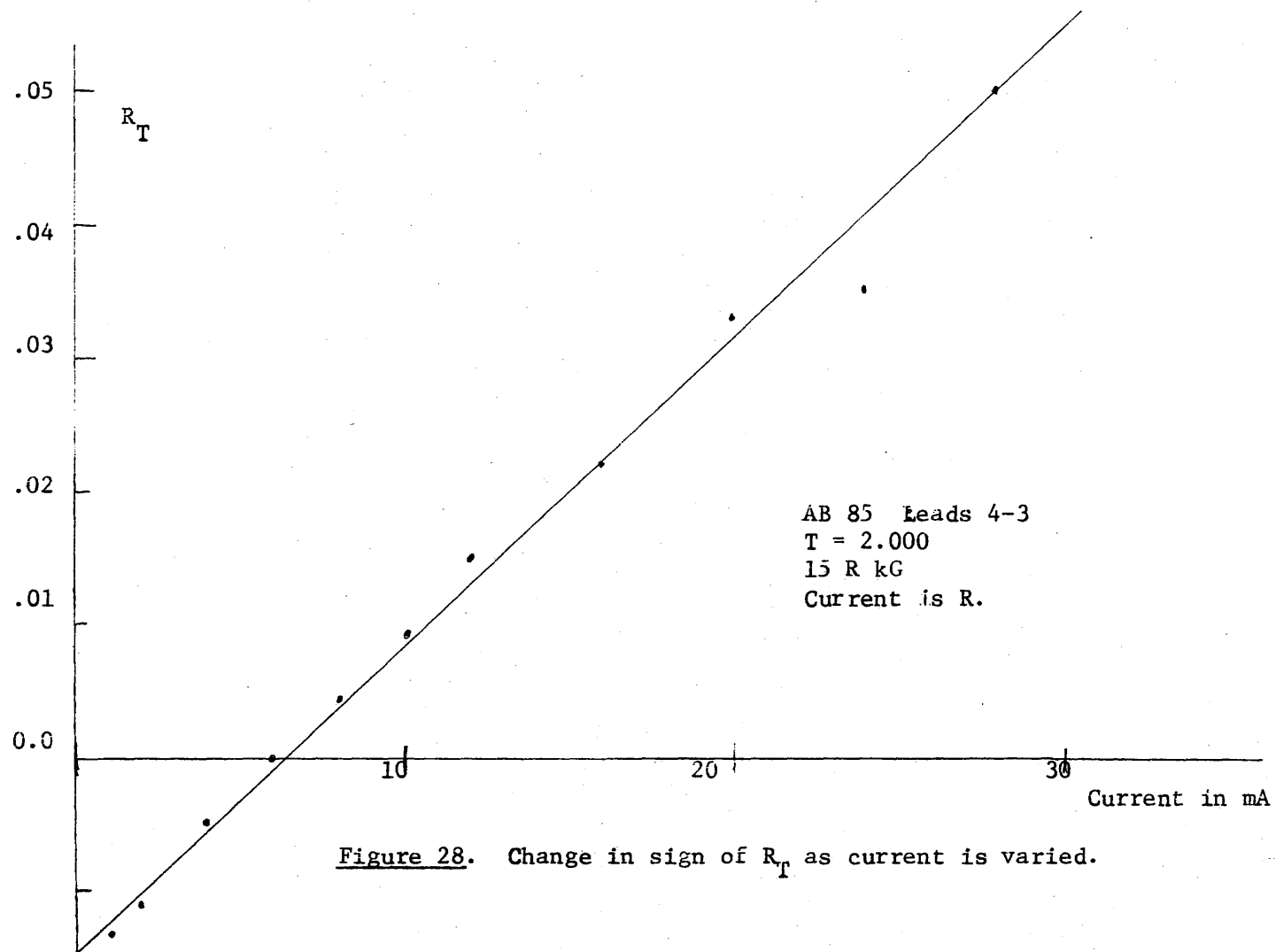
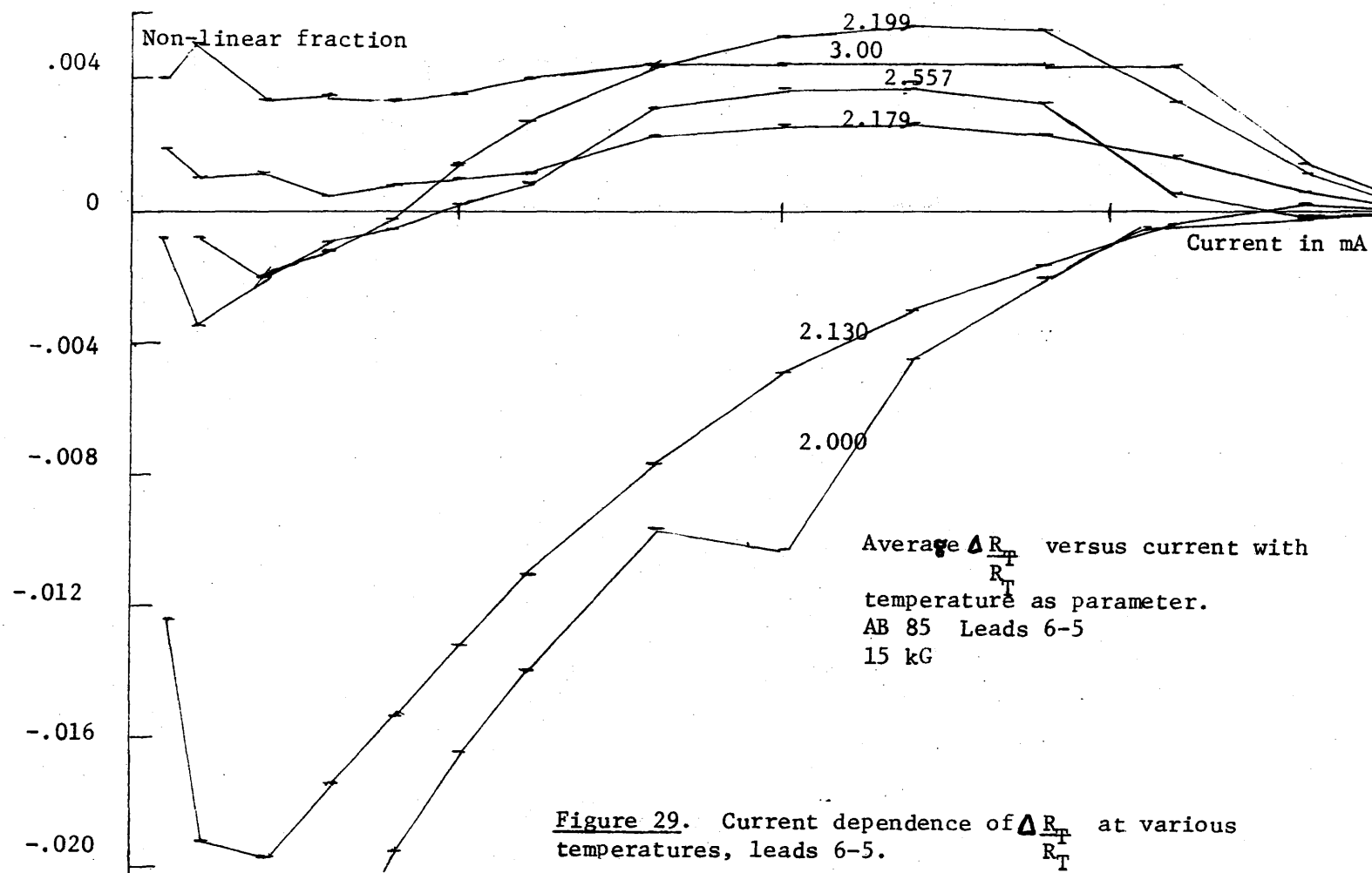
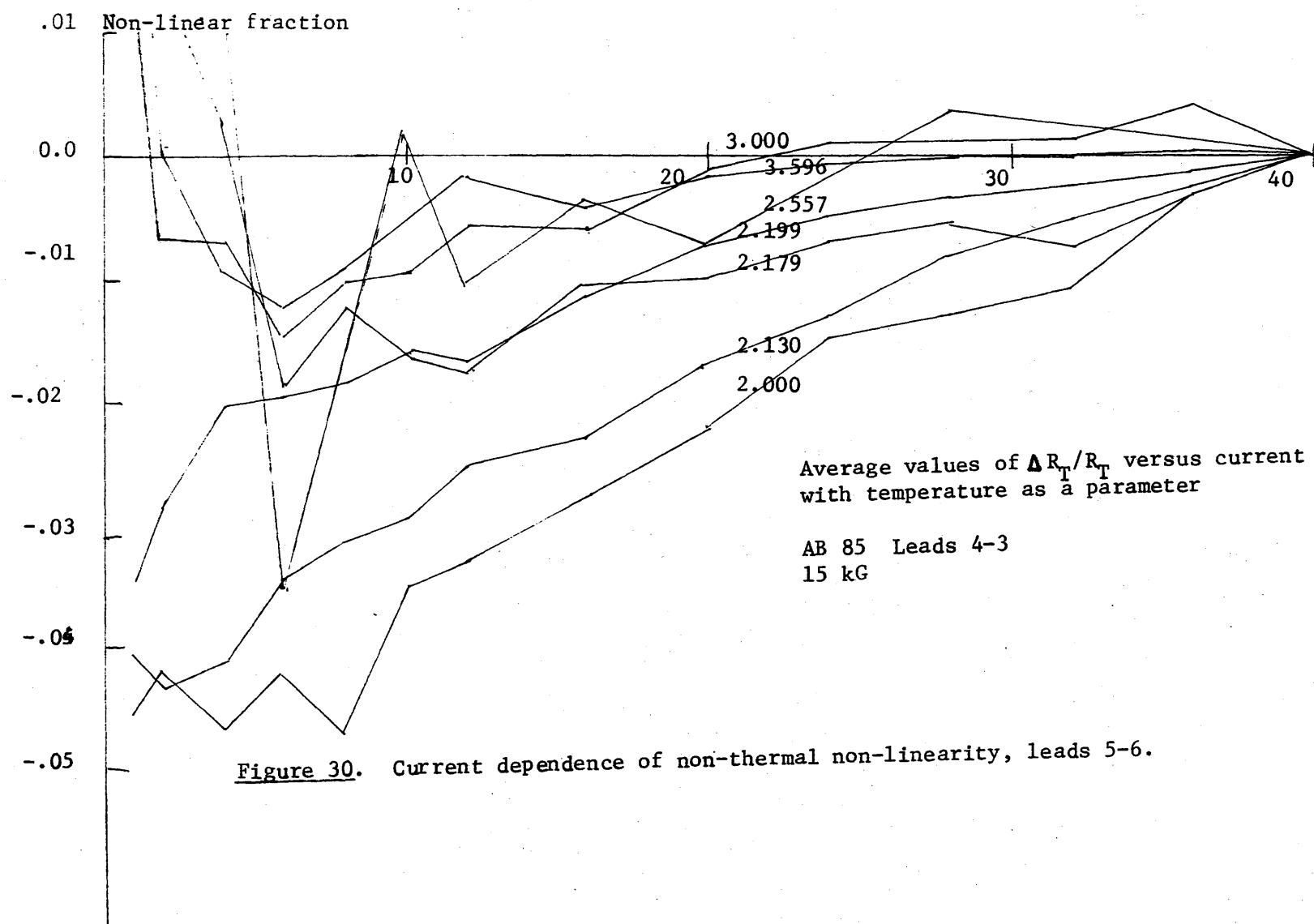


Figure 28. Change in sign of R_T as current is varied.





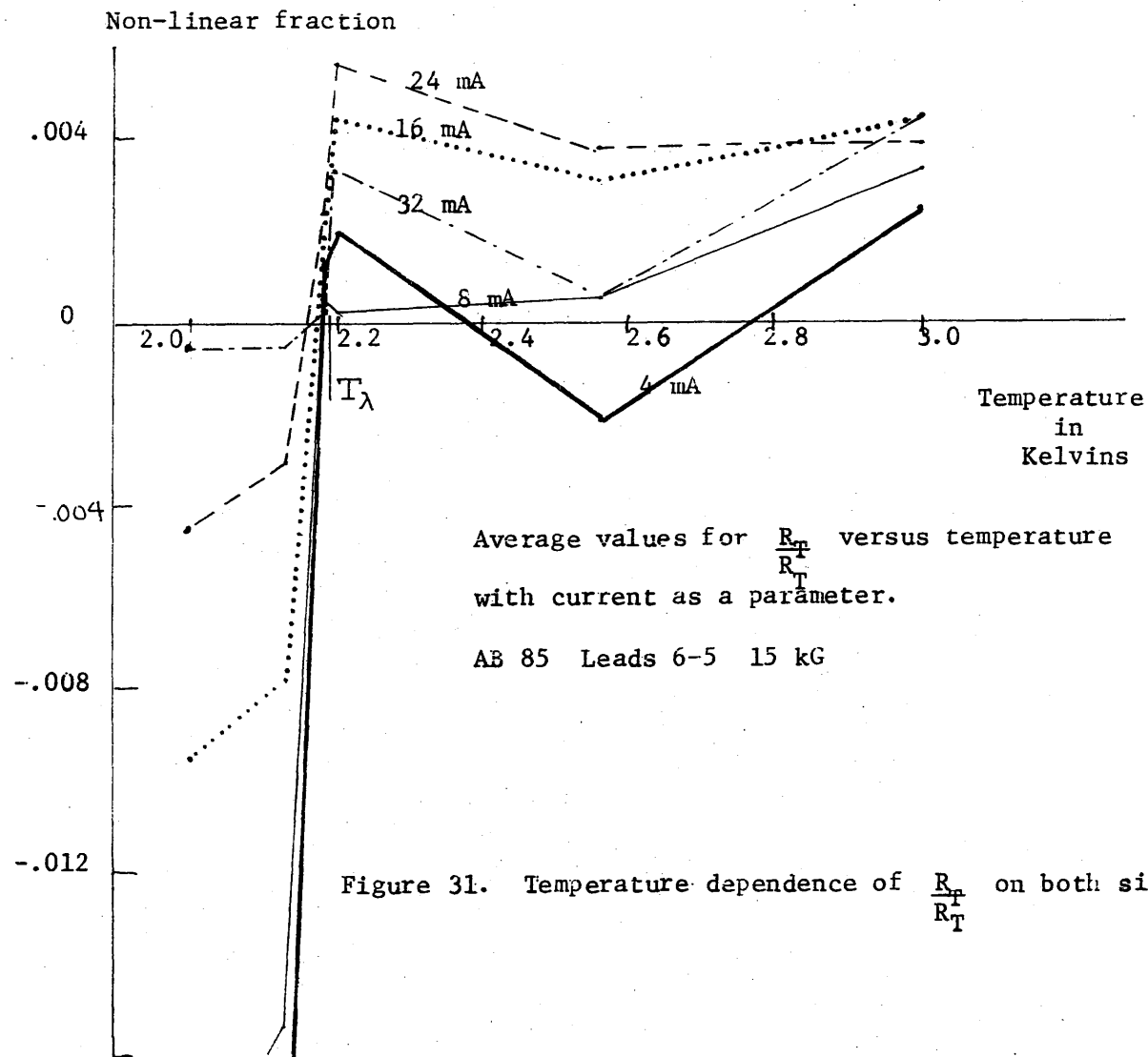
presented. Even though the size of $\Delta R/R$ for some combinations might vary over a wide range, the averages are in surprisingly close agreement. This tends to further reinforce the feeling that the effect being seen is intrinsic in nature, and is a function of the crystal itself.

The possible source of such an intrinsic non-ohmicity is at present unclear. As has already been mentioned, the Esaki kink, and the self field effects are more or less discounted, because of the different experimental conditions they require. The quantum size dependence has never been mentioned in so large a crystal, and the expressions used (14) do not seem to predict it. One size effect, described by Hattori (15) as a "diffusion size effect" is a possible explanation. The article does not seem to predict a current dependence of the effect, but mentions it as a possible explanation for some presently unavailable non-ohmic results (16). To resolve the size dependence of the effect, some careful sample construction must be initiated, and data taken from crystals sufficiently equivalent to enable the size dependence of our intrinsic effect to be measured. If such a research plan were adopted, the most logical temperature range would be in the superfluid region, because the thermal problems are so much reduced by the infinite thermal conductivity of the bath.

One of the stated goals of the pulsed data research was to separate the non-linearity into two precise parts. The existence of some thermal component had been well demonstrated before the

pulse work, but was only able to be clearly viewed when examined as a function of time. The attempt to demonstrate the existence of an intrinsic effect clearly hinged on keeping the bath from warming, lest the thermal problems overshadow the intrinsic effect. This warming would be noted first by the steepness of the trace even of a short pulse, but also perhaps by a net negative curvature to graph $\Delta R/R$ versus I . The most rigorous proof of existence for an intrinsic non-ohmic effect would be a continuity of the short pulsed non-linearity across the lambda point of the bath, since the thermal conduction properties of the environment change so drastically at that point.

The graphs of $\Delta R/R$ versus temperature with current as a parameter are reproduced in Figures 31 and 32. It is obvious that the goal of continuity across the lambda transition has not been fully reached. On the other hand, leads 4 and 3 indicate some success in separation. From this graph one might conclude that the separation is indeed nearly complete, but Figure 30 indicates otherwise. Note that at the two temperatures well below the lambda point the curves show a distinctly more linear current dependence of $\Delta R_T/R_T$ than those for temperatures greater than 2.175 K. It is suspected, then, that this linear current dependence would be similar in the normal fluid, and would account for the positive slope of the $\Delta R_T/R_T$ curve at low currents. At the higher currents the Joule heating begins to predominate in spite of the short duty cycle adopted, and the negative curvature seen in all the high temperature curves is the result.



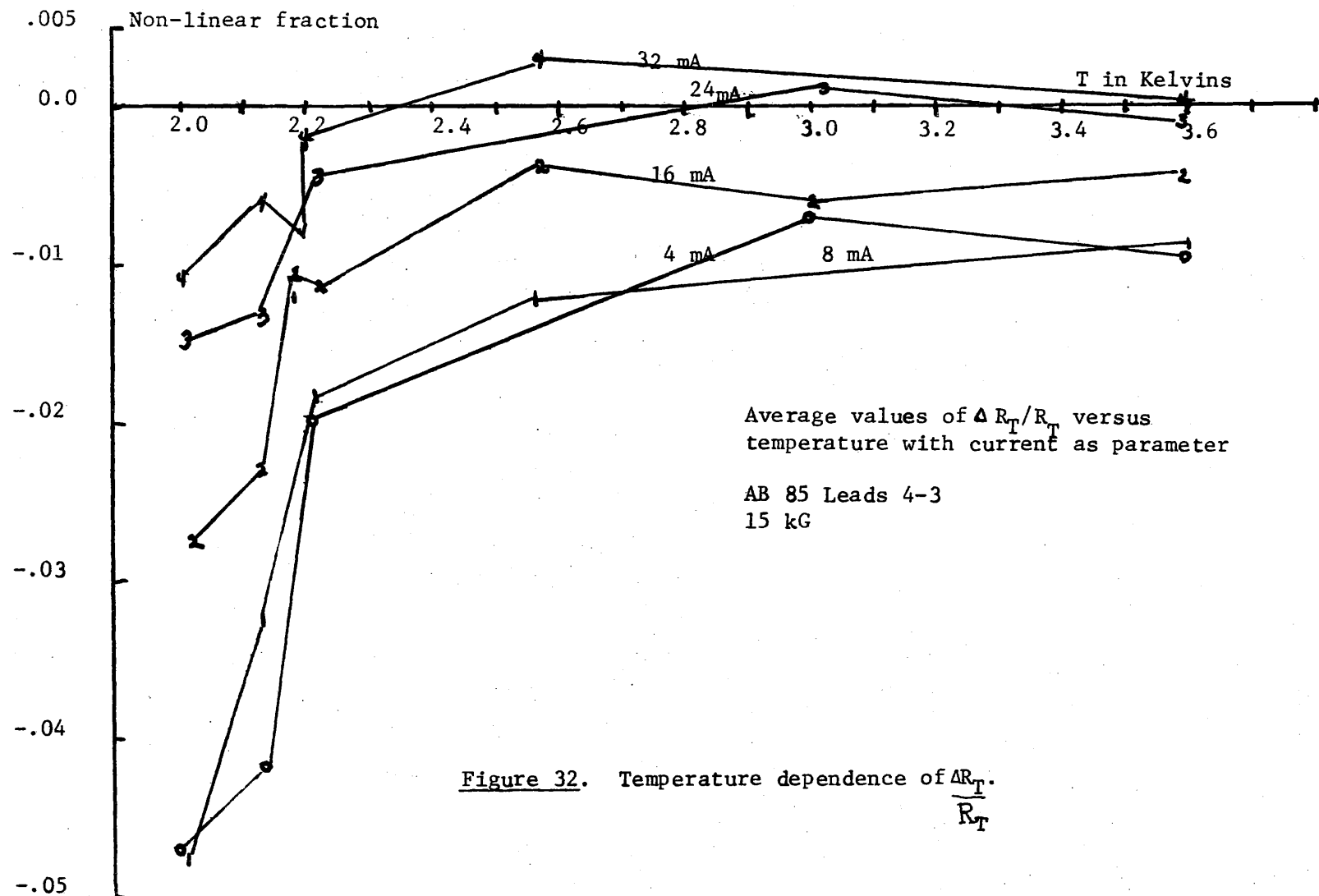


Figure 32. Temperature dependence of $\frac{\Delta R_T}{R_T}$.

CONCLUSIONS AND RECOMMENDATIONS

Conclusions

Longitudinal and transverse voltages in bismuth have been found to depart from relations so simple as Ohm's law between voltage and current. Part of the departure has been shown to be thermal in origin, and has been seen to have a rather peculiar time dependence. An intrinsic non-ohmic effect has also been shown to contribute to a smaller degree to the non-linearity observed by a DC potentiometer. Below the lambda point, the effects of heating have been separated from the intrinsic effect, but a discontinuity in the short-pulse results at the lambda point implies that heating has not been completely eliminated for the situation in which the crystal was immersed in normal fluid. Several models have been proposed for these effects but those amenable to calculation have not explained the experimental results.

Recommendations

Thermal Non-linearity. The principal objective to be determined with respect to the thermal question is to obtain some mechanism for the observed peak. The most attractive hypothesis at present seems to be a delayed bubble nucleation model, so some work could be spent on testing it. The first requisite would be some comprehensive data gathering, using a point by point average of the four combinations of field orientations, and finding the temperature and current

dependence of the parameters of the peak. To directly test for the delayed bubbling, perhaps the coherent noise effect could be used. A loop could be constructed, only one of the sides of which would be free to move. Mounted next to the crystal, the vibrations it sensed from the bubbles would generate a voltage which could be observed on the oscilloscope. Although a negative result to this experiment could not disprove the hypothesis, a positive one would certainly confirm it.

Another test of the bubbling hypothesis would be to cool the bath by pumping on it, and suppress the boiling by repressurizing faster than the temperature can rise. If the peak were indeed dependent on nucleation, the lack of a saturated vapor pressure over the liquid ought to modify the peak drastically.

Should the bubbling hypothesis not be confirmed by these experiments, some study could be made of the effects on the peak of changing the sample surface. Smoothing or roughing the face of the crystal should both have drastic effects on the availability of sites for nucleation, and the degree to which superheating could occur.

Non-thermal Effect. The item of highest priority regarding this effect is to eliminate completely the thermal component. It is hoped that a lower duty cycle could do this, and perhaps only single pulses should be used. It might be necessary with single pulses to use a more precise temperature control to eliminate possible temperature drift between readings.

Even if it proves impossible to completely separate the non-thermal component above the lambda point, in the superfluid phase where thermal problems are less severe some more careful experiments should be done on the size and magnetic field dependence of the intrinsic non-ohmicity.

A SELECTED BIBLIOGRAPHY

1. Hall, E.H. 1879, "On a New Action of the Magnet on Electric Currents", American Journal of Mathematics, vol. 2, pp. 287-292.
2. Esaki, Leo. "New Phenomenon in Magnetoresistance of Bismuth at Low Temperatures", Physical Review Letters, vol. 2, no. 1, p. 4, 1962.
3. Jaggi, R. and R. Sommerhalder. "Hall-Effekt und Eigen-Hall Effekt in Normal- und Supraleitern", Helvetica Physica Acta, vol. 32, pp. 167-196, 1959.
4. Ziman, J.M. Electrons and Phonons, Oxford Univ. Pr. p. 486, 1960.
5. Marcus, J.A. "Oscillatory Hall Effect and Magnetoresistance of Bismuth", a paper read at the American Physical Society meeting, Baltimore, March 17, 1955.
6. Weiner, D. "De Haas - Van Alphen Effect in Bismuth-Tellurium Alloys", Physical Review, vol. 125, no. 4, pp. 1226-1238, 1962.
7. James F. Scanlon Co., 11701 E. Washington Blvd., Whittier California, 90606.
8. Zemansky, M.W. Heat and Thermodynamics, McGraw Hill, 1957, p. 381.
9. Little, W.A. "Kapitza Resistance Between Helium and Metals in the Normal and Superconducting States", Physical Review, vol. 123, no. 2, p. 435, 1961.
10. Brodie, L.C., C.L. Hartley and W.E. Nordgren, unpublished data, 1964.
11. Pollack, G.L. "Kapitza Resistance", Reviews of Modern Physics, vol. 41, no. 1, 1969.
12. Hartley, C.L. private communication, 1966.
13. Ahlers, G. "Effect of the Gravitational Field on the Superfluid Transition in He⁴", Physical Review, vol. 171, no. 1, pp. 275-282, 1968.

14. Yu, F. Ogrin, V.N. Lutsii and M.T. Elinson, "Quantum Size Dependence in Thin Bismuth Films", Journal of Experimental and Theoretical Physics Letters, vol. 3, 1966.
15. Hattori, T. "Diffusion Size Effect in Bismuth at Liquid He Temperatures", Journal of the Physical Society of Japan, Vol. 123, no. 1, p. 19, 1967.
16. Hattori, T. Journal of the Physical Society of Japan, vol. 18, p. 1294, 1963.
17. Takeo, M. private communication, 1964.

APPENDIX A

AVERAGE TEMPERATURE CALCULATION

The continuity equation for the flow of heat in the presence of a source \dot{Q} is

$$\nabla \cdot \mathbf{j} + \dot{q} = \dot{Q} \text{ source}$$

where j is the density of the thermal current" and \dot{q} is the rate of change of "heat density" in a differential volume. The heat transport equation may be written

$$\mathbf{j} = -\kappa \nabla T, \text{ where } \kappa \text{ is}$$

thermal conductivity. Taking

Figure 33. Dimensions for average temperature calculation

the divergence of the

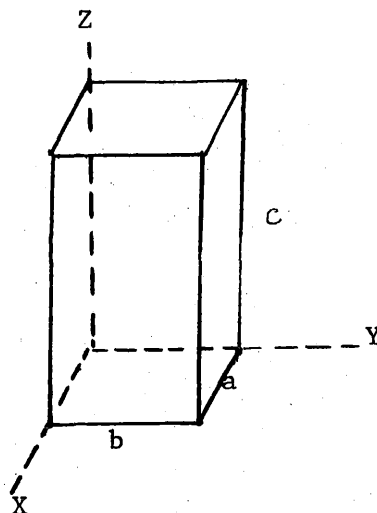
transport equation, and letting the source be Joule heat due to current J through a medium of conductivity σ .

$$\nabla \cdot \mathbf{j} = -\kappa \nabla^2 T = \frac{\partial Q}{\partial t} = -\frac{J^2}{\sigma}$$

when a steady state has been established.

If c is much longer than a or b , we may neglect the vertical direction, and only consider heat flow through the faces. Using a two dimensional Fourier expansion for the temperature distribution:

$$T = T_0 + \sum_{l,m} A_{l,m} \sin\left(\frac{l\pi x}{a}\right) \sin\left(\frac{m\pi y}{b}\right)$$



Then

$$\nabla^2 T = \sum_{l,m} A_{lm} \pi^2 \left(\frac{l^2}{a^2} + \frac{m^2}{b^2} \right) \sin \left(\frac{l\pi x}{a} \right) \sin \left(\frac{m\pi y}{b} \right) = \frac{J^2}{\kappa \sigma}$$

the coefficients A_{lm} are therefore given by

$$A_{lm} = \frac{J^2}{\sigma \kappa} \frac{2^4}{\pi^4} \left(lm \left(\frac{l^2}{a^2} + \frac{m^2}{b^2} \right) \right)^{-1}, \text{ where } l \text{ and } m \text{ must}$$

be added and if $\Delta T(x,y)$ is the amount that the temperature at (x,y) rises above the bath temperature.

$$\Delta T = \sum_{lm} \frac{J^2}{\sigma \kappa} \frac{2^4}{\pi^4} \left(lm \left(\frac{l^2}{a^2} + \frac{m^2}{b^2} \right) \right)^{-1} \sin \left(\frac{l\pi x}{a} \right) \sin \left(\frac{m\pi y}{b} \right)$$

To find the amount the average temperature may rise above that of the bath, we average the ΔT over the crosssectional area:

$$\begin{aligned} \overline{\Delta T} &= \frac{1}{ab} \int_0^a \int_0^b \Delta T \, dx dy = \\ &= \frac{1}{ab} \cdot \frac{J^2}{\sigma \kappa} \cdot \frac{2^4}{\pi^4} \sum_{lm} \int_0^a \int_0^b \left(lm \left(\frac{l^2}{a^2} + \frac{m^2}{b^2} \right) \right)^{-1} \sin \left(\frac{l\pi x}{a} \right) \sin \frac{m\pi y}{b} \, dx dy \end{aligned}$$

Integrating, we have:

$$\begin{aligned} &= \frac{1}{ab} \cdot \frac{J^2}{\sigma \kappa} \cdot \frac{2^4}{\pi^4} \left(lm \left(\frac{l^2}{a^2} + \frac{m^2}{b^2} \right) \right)^{-1} \frac{ab}{lm} \frac{2^2}{\pi^2} \\ &= \frac{J^2}{\sigma \omega} \frac{2^6}{\pi^6} \sum_{lm} \left(l^2 m^2 \left(\frac{l^2}{a^2} + \frac{m^2}{b^2} \right) \right)^{-1} \end{aligned}$$

A typical set of values in these experiments is:

$$\frac{J^2}{\sigma \kappa} = \left(\frac{I^2 R}{\text{volume}} \right) = \left(\frac{(0.05)^2 \cdot 6}{3 \times 4 \times 1.5 \times 10^9} \right) \frac{W}{m^3} \kappa = 1750. \, W/m-K$$

The sum becomes $2.09 \times 10^{-6} m^{-2}$, and $\overline{\Delta T} = 6 \times 10^5 \, K$.

APPENDIX B

SELF INDUCED MAGNETIC FIELD CALCULATION

Jaggi and Sommerhalder (3) derive the following equation for the self magnetic field, induced in an infinitely long parallelepiped with rectangular cross-section:

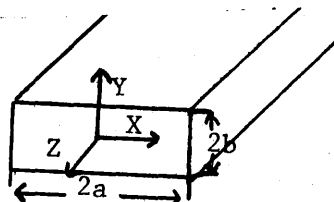


Figure 34. Dimensions for self field calculation.

$$H_y = \frac{Jz}{4\pi} \left[(y+b) \ln \frac{(x-a)^2 + (y+b)^2}{(x-a)^2 + (y-b)^2} + (y-b) \ln \frac{(x-a)^2 + (y-b)^2}{(x+a)^2 + (y-b)^2} \right. \\ \left. + 2(x+a) \left\{ \tan^{-1} \left(\frac{y+b}{x+a} \right) - \tan^{-1} \left(\frac{y-b}{x+a} \right) \right\} \right. \\ \left. + 2(x-a) \left\{ \tan^{-1} \left(\frac{y-b}{x-a} \right) - \tan^{-1} \left(\frac{y+b}{x-a} \right) \right\} \right]$$

A typical configuration for our crystals would be:

$$a = 2\text{mm}, b = .5\text{mm} \quad I = Jz \quad 4ab = 50 \text{ mA}$$

maximum field, at the corner of the crystal ($x=a, y=b$)

$$H_y = \frac{5 \times 10^2 \text{ A}}{4\pi \times 2 \times 10^{-3} \text{ m}} \cdot .5 \times 4 \times 10^{-3} \text{ cm}^2 \left[(10^3 \text{ m}) \ln \frac{17 \times 10^6 \text{ m}^2}{10^6 \text{ m}^2} \right. \\ \left. + 8 \times 10^3 \text{ m} \left\{ \tan^{-1} \frac{1}{4} - \tan^{-1} 0 \right\} \right] \\ = 3.18 \frac{\text{A}}{\text{m}} \frac{4\pi}{10^8} = 3.99 \times 10^2 \text{ G}$$

The current of 50 mA produces a .04 G field at the corner of a 1 x 4 mm crystal, which is ~2 ppm in 15 kG.

APPENDIX C

COHERENT NOISE CALCULATION

The hypothesis which was suggested for the phenomenon of coherent noise was that a closed loop was being formed by the pair of potential leads, the crystal, their connection to the amplifiers and the input impedances of the amplifiers. In the very strong magnetic field, a very small change in the area of the loop would cut a large number of flux lines and hence generate a voltage. Since the input impedance is so high for the amplifiers we use, almost all voltage generated in the circuit would appear across the terminals of the amplifiers and be fed to the oscilloscope for display. It is easy to calculate how small the motion of the leads need be to generate such a voltage.

Let us take the dimensions of AB 85 as an instance: The crystal itself is 4.8 mm wide, and another millimeter should be added between where the lead is welded and where the lead is first glued. At a frequency of perhaps 700 Hz, this results in a trace on our oscilloscope of about 2 mV peak to peak amplitude.

Now since $V = \dot{\phi} = -B\dot{A}$ we can write $\dot{A} = \frac{V}{B}$ and let us assume $A(t)$ is of the form $A = A_0 e^{i\omega t} + A_{\text{static}}$ so $\dot{A} = i\omega A_0 e^{i\omega t}$ and since $V = V_0 e^{i\omega t}$ we have $\omega A_0 e^{i\omega t} = \frac{V_0 e^{i\omega t}}{B}$. Therefore $A_0 = \frac{V_0}{\omega B}$, and plugging in appropriate values for the variables:

$$A_o = \frac{1mV}{2 \pi 60 \text{ (amplifications)}} \cdot 700 \text{ Hz} \cdot 1.5 \omega/m^2 = 2.5 \times 10^{-9} m^2$$

In the geometry of AB 85, this reduces to a lateral amplitude of the potential lead vibration of approximately .0036 mm. As a point of reference, the leads are about .09 mm in diameter, which implies rather small vibrations.